Inorganic Chemistry

Article

pubs.acs.org/IC

Synthesis, Structural Characterization, Photophysical, Electrochemical, and Anion-Sensing Studies of Luminescent Homo- and Heteroleptic Ruthenium(II) and Osmium(II) Complexes Based on Terpyridyl-imidazole Ligand

Chanchal Bhaumik, Debasish Saha, Shyamal Das, and Sujoy Baitalik*

Department of Chemistry, Inorganic Chemistry Section, Jadavpur University, Kolkata 700032, India

Supporting Information

ABSTRACT: A series of hetero- and homoleptic tridentate ruthenium(II) and osmium(II) complexes of compositions $[(tpy\text{-}PhCH_3)Ru(tpy\text{-}HImzphen)](ClO_4)_2$ (**1**), $[(H_2pbbzim)\text{-}Ru(tpy\text{-}HImzphen)](ClO_4)_2$ (**2**), and $[M(tpy\text{-}HImzphen)_2]\text{-}(ClO_4)_2$ [M = Ru^{II} (**3**) and Os^{II} (**4**)], where tpy-$PhCH_3$ = 4′-(4-methylphenyl)-2,2′:6′,2″-terpyridine, H_2pbbzim = 2,6-bis-(benzimidazole-2-yl)pyridine and tpy-HImzphen = 2-(4-[2,2′:6′,2″]terpyridine-4′-yl-phenyl)-1*H*-phenanthro[9,10-*d*]-imidazole, have been synthesized and characterized by using standard analytical and spectroscopic techniques. X-ray crystal structures of three complexes **2**, **3**, and **4** have been determined. The absorption spectra, redox behavior, and luminescence properties of the complexes have been thoroughly investigated. All of the complexes display moderately strong luminescence at room temperature with lifetimes in the range of 10−55 ns. The effect of solvents on the absorption and emission spectral behavior of the complexes has also been studied in detail. The anion sensing properties of all the complexes have been studied in solution using absorption, emission, and ^{1}H NMR spectral studies and by cyclic voltammetric (CV) measurements. It has been observed that the complexes **1**, **3**, and **4** act as sensors for F^-only, whereas **2** acts as sensor for F^-, AcO^-, and to some extent for $H_2PO_4^-$. It is evident that in the presence of excess of anions deprotonation of the imidazole N−H fragment(s) occurs in all cases, an event which is signaled by the development of vivid colors visible with the naked eye. The receptor−anion binding/equilibrium constants have been evaluated.

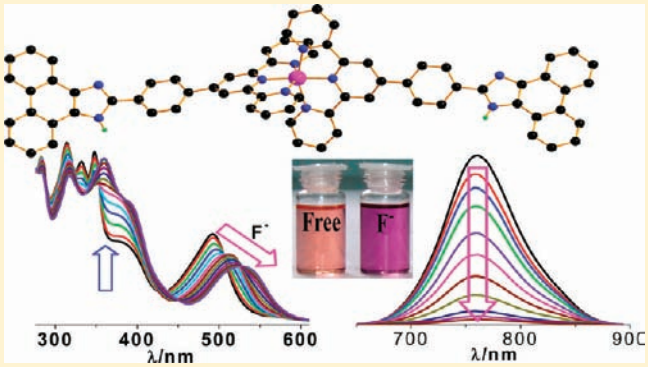

INTRODUCTION

Ruthenium(II) and osmium(II) complexes with polypyridyl ligands have been the subject of numerous studies because of their unique combination of spectroscopic, photophysical, photochemical, and electrochemical properties.[1] These properties often can be tuned by ramification of ligand structures and by introducing coligands in complexes. Consequently, these complexes are potentially useful in many important areas of research such as photochemical conversion of solar energy, catalytic conversion of water to molecular oxygen, molecular electronic devices, and photoactive DNA cleavage for therapeutic purposes.[2] Thus, to be effective, such complexes should exhibit a metal-to-ligand charge transfer (MLCT) band at relatively higher wavelengths, and the lifetime of the ^{3}MLCT state should be long, the quantum yield of $^1O_2$ should be high, and the oxidation potential of the excited state should be relatively low. Among the most widely studied complexes, particularly popular are ruthenium complexes derived from bipyridine-type of ligands. Many complexes of this type (such as $[Ru(bpy)_3]^{2+}$, bpy = 2,2′-bipyridine) are of interest because they absorb a significant portion of the visible spectrum, have relatively long-lived excited states (>1 μs), are often stable following one-electron oxidation and reduction, and exhibit good photochemical stability.[1] The equilibrated excited state of these complexes has been assigned as a MLCT state. However, the synthesis of tris(bpy)-based complexes is hampered by the mixtures of diasteromers that form because of their Δ and Λ enantiomers.[3] In contrast to $[Ru(bpy)_3]^{2+}$ type complexes, structurally more appealing $[Ru(tpy)_2]^{2+}$ type complexes give rod-like assemblies when substituted at the 4′-position of the tpy ligands.[4] However, usually such complexes are practically non-luminescent at room temperature, and their excited state lifetime (τ = 0.25 ns)[5] is also very short and therefore are the major deterrent for them to act as photosensitizer. Consequently, much effort has been devoted to design and synthesize tridentate polypyridine ligands that can produce ruthenium(II) complexes with enhanced emission quantum yields and excited-state lifetimes. Most of the approaches aim to increase the energy gap between the radiative ^{3}MLCT and quenching ^{3}MC states. Stabilization of the ^{3}MLCT state can be achieved inter alia by substitution of the tpy ligands by

Received: July 27, 2011
Published: November 18, 2011

electron-withdrawing groups,[6] introducing coplanar a hetero-aromatic moiety,[7] incorporation of organic chromophore, and so forth. Indeed, such approaches have produced complexes that have longer emission lifetimes compared to the parent compounds.[8−10] A second approach is to destabilize the ^{3}MC state by using cyclometalated ligands.[11−13] One can also modify the terpyridine directly, by replacing the pyridines with other heterocyclic rings to enlarge the bite angle of the tridentate ligand.[14]

To this end, we report herein a series of luminescent bis-tridentate ruthenium(II) and osmium(II) complexes by using newly synthesized and characterized 2-(4-[2,2′:6′,2″]-terpyridine-4′-yl-phenyl)-1*H*-phenanthro[9,10-*d*]imidazole (tpy-HImzphen) system, wherein a *p*-tolylterpyridine moiety has been fused at its 4′-position with a phenanthrene-imidazole motif. To allow fine-tuning of the electronic properties, several homo- and heteroleptic complexes have been synthesized, resulting in four complexes as shown in Chart 1. The most striking feature of this class of compounds is that they are luminescent at room temperature in fluid solutions. The introduction of the tridentate ligand, tpy-HImzphen, results in an enhancement of the excited-state lifetime by as much as 2 orders of magnitude with respect to the parent $[Ru(tpy)_2]^{2+}$ complex. Additionally, these complexes also have varying number of imidazole NH protons which can be utilized for sensing and recognizing selective anions either via hydrogen bonding interaction or by proton transfer. Development of a multi-channel metalloreceptor for selective anions has emerged as topic of intensive studies because of their important roles in biological, aquatic, environmental, and industrial processes.[15−21] When the metalloreceptor is designed to function as a sensor, metal fragments can be used as reporter units for modulating a signal, usually color, fluorescence, or electrochemical potentials, as a result of host−guest interaction.[17−24] Interestingly, the present complexes owing to the presence of varying number of imidazole NH protons which became appreciably acidic because of metal coordination can be utilized for multi-channel recognition of ions such as F^- and AcO^- ions in solution. As will be seen, consequent to anion interaction, remarkable changes in color (visible with open eyes) along with similar absorption, photoluminescence, and redox responses occur.

Chart 1

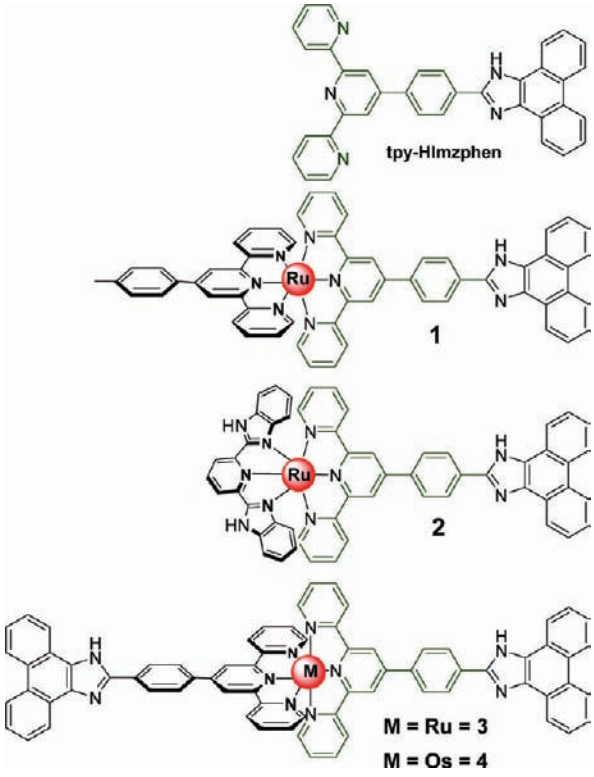

EXPERIMENTAL SECTION

Materials. Reagent grade chemicals obtained from commercial sources were used as received. Solvents were purified and dried according to standard methods. 4′-(4-methylphenyl)-2,2′:6′,2″-terpyridine (tpy-PhCH$_3$), 4′-(*p*-bromomethylphenyl)-2,2′:6′, 2″-terpyridine (tpy-PhCH$_2$Br), 4′-(*p*- dibromomethylphenyl)-2,2′:6′,2″-terpyridine (tpy-PhCHBr$_2$),[22a,25] [4′-(*p* -triphenylphosphoniummethylphenyl)-2,2′:6′,2″-terpyridine] bromide (tpy-PhCH$_2$PPh$_3$Br), 4′-(*p*-formylphenyl)-2,2′:6′,2″-terpyridine (tpy-PhCHO),[26] and 2,6-bis-(benzimidazole-2-yl)pyridine (H$_2$pbbzim)[27] were synthesized according to the literature procedures. [(tpy-PhCH$_3$)RuCl$_3$] and [(H$_2$pbbzim)RuCl$_3$] were prepared by reaction of RuCl$_3$·3H$_2$O with tpy-PhCH$_3$ and H$_2$pbbzim in 1:1 molar ratio in refluxing ethanol.

Preparation of the Ligand. *2-(4-[2,2′:6′,2″]terpyridine-4′-yl-phenyl)-1H-phenanthro[9,10-d]imidazole (tpy-HImzphen).* 4′-(*p*-formylphenyl)-2,2′:6′,2″-terpyridine (tpy-PhCHO) (337 mg, 1.00 mmol), 9,10-phenanthrenedione (230 mg, 1.10 mmol), and ammonium acetate (1.6 g, 20 mmol) were stirred in acetic acid (30 mL), and the mixture was refluxed for 2 h with continuous stirring. On cooling to room temperature a pale yellow crystalline compound deposited. The resulting compound was collected by filtration and washed several times with water and then air-dried. The compound was finally recrystallized from chloroform-ethanol (1:1) mixture, and the desired compound was obtained as light yellow crystalline solid (370 mg, 0.70 mmol, yield 70%). ^{1}H NMR {500 MHz, DMSO−d_6, δ(ppm)}: 13.60 (s, 1H, NH imidazole), 8.86 (d, 2H, J = 8.5 Hz, H9), 8.82 (s, 2H, H3′), 8.79 (d, 2H, J = 4.0 Hz, H6), 8.69 (d, 2H, J = 8.0, H3), 8.60 (d, 2H, J = 8.0 Hz, H12), 8.53 (d, 2H, J = 8.0 Hz, H8), 8.20 (d, 2H, J = 8.5 Hz, H7), 8.05 (t, 2H, J = 7.5 Hz, H4), 7.75 (t, 2H, J = 7.5 Hz, H11), 7.65 (t, 2H, J = 7.7 Hz, H10), 7.54 (t, 2H, J = 6.0 Hz, H5). ESI-MS: m/z 525.51 ([L+H]$^+$). Anal. Calcd for $C_{36}H_{23}N_5$: C, 82.26; H, 4.41; N, 13.32. Found: C, 82.18; H, 4.44; N, 13.29.

Synthesis of the Metal Complexes. The complexes were prepared under oxygen and moisture free dinitrogen using standard Schlenk techniques.

[(tpy-PhCH$_3$)Ru(tpy-HImzphen)](ClO$_4$)$_2$·2H$_2$O (1). A mixture of Ru(tpy-PhCH$_3$)Cl$_3$ (75 mg, 0.14 mmol), AgBF$_4$ (92 mg, 0.47 mmol), and 30 mL of acetone were refluxed with continuous stirring for 4 h. After the solution cooled down to room temperature, the precipitated AgCl was removed by filtration. A 40 mL portion of EtOH was then added to the filtrate. Acetone was removed by rotary evaporation. To the resulting solution, solid powdered ligand (80 mg, 0.15 mmol) was added and refluxed for 12 h with continuous stirring. During cooling down to room temperature a deep red compound deposited. The resulting compound was filtered, washed with chloroform and ether, and then dried under vacuum. The compound was redissolved in a minimum volume of acetonitrile and then subjected to silica-gel column chromatography (eluent: acetonitrile). The eluent was rotary evaporated to small volume and then anion exchange reaction with NaClO$_4$ gave rise to the desired compound. The compound was finally recrystallized from acetonitrile−methanol (1:1) mixture in presence of a few drops of aqueous 10^{-4} M perchloric acid (110 mg, Yield: 70%). Anal. Calcd. for $C_{58}H_{44}N_8Cl_2O_{10}Ru$: C, 58.79; H, 3.74; N, 9.46. Found: C, 58.77; H, 3.76; N, 9.44. ^{1}H NMR data {300 MHz, DMSO-d_6, δ(ppm)}: 13.71 (s, 1H, NH imidazole), 9.59 (s, 2H, H3′), 9.47 (s, 2H, H3″), 9.13 (t, 4H, J = 9.5 Hz, H6), 8.94−8.84 (m, 2H, H9), 8.69−8.61 (m, 6H, 2H7 + 2H8 + 2H12), 8.37 (d, 2H, J = 8.1 Hz, H8′), 8.12−8.04 (m, 4H, H4), 7.84−7.76 (m, 2H, H11), 7.73−7.66 (m, 2H, H10), 7.58−7.57 (m, 6H, 4H3 + 2H7′), 7.32−7.27 (m, 4H, H5), 2.48

dx.doi.org/10.1021/ic201610w | *Inorg. Chem.* 2011, 50, 12586−12600

(s, 3H, CH_3). ESI-MS (positive, CH_3CN) m/Z = 475.53 (100%) $[(tpy\text{-}PhCH_3)Ru(tpy\text{-}HImzphen)]^{2+}$. UV−vis [DMSO; λ_{max}, nm (ε, M^{-1} cm^{-1})]: 502 (37350), 390 (27760), 316 (71000), 285 (73700).

[(H_2pbbzim)Ru(tpy-HImzphen)](ClO_4)$_2$·2H_2O (2). [(H_2pbbzim)$RuCl_3$] (75 mg, 0.14 mmol) was suspended into ethylene glycol (30 mL) and heated at 100 °C with continuous stirring. To the suspension was added the ligand, tpy-HImzphen (80 mg, 0.15 mmol), and the reaction mixture was again heated at 180 °C for 24 h. The resulting solution was cooled, and the perchlorate salt of the complex was precipitated by pouring the solution into an aqueous solution of $NaClO_4·H_2O$ (1.0 g in 10 mL of water). The precipitate obtained was filtered and washed with water and dried under vacuum. The compound was then purified by silica gel column chromatography using a mixture of CH_3CN and 10% aqueous KNO_3 (10:1) as the eluent. Subsequent anion exchange reaction with $NaClO_4·H_2O$ gave rise the desired compound. The compound was finally recrystallized from acetonitrile−methanol (1:1) mixture in presence of a few drops of aqueous 10^{-4} M perchloric acid (105 mg, Yield: 65%). Calcd. for $C_{55}H_{40}N_{10}Cl_2O_{10}Ru$: C, 56.32; H, 3.44; N, 11.94 Found: C, 56.30; H, 3.47; N, 11.91. ^{1}H NMR data {300 MHz, DMSO-d_6, δ(ppm)}: 15.03 (s, 3H, NH imidazole), 9.68 (s, 2H, H3′), 9.06 (d, 2H, J = 8.1 Hz, H6), 8.92 (d, 2H, J = 8.3 Hz, H9), 8.85 (d, 2H, J = 8.5 Hz, H8), 8.78 (d, 2H, J = 8.0 Hz, H7), 8.74−8.60 (m, 5H, 1H10′+2H11′+2H12), 7.97 (t, 2H, J = 7.4 Hz, H4), 7.82 (t, 2H, J = 7.4 Hz, H11), 7.71 (t, 2H, J = 7.3 Hz, H10), 7.67 (d, 2H, J = 8.3 Hz, H3), 7.50 (d, 2H, J = 5.2 Hz, H12′), 7.30−7.23 (m, 4H, 2H5 + 2H13), 7.03 (t, 2H, J = 7.8 Hz, H14), 6.10 (d, 2H, J = 8.3 Hz, H15). ESI-MS (positive, CH_3CN) m/Z = 469.13 (100%) $[(H_2pbbzim)Ru(tpy\text{-}HImzphen)]^{2+}$; 937.19 (31%) [(pbbzim)Ru(tpy-HImzphen)]. UV−vis [MeCN; λ_{max}, nm (ε, M^{-1} cm^{-1})]: 492 (27280), 382 (24810), 348 (51790), 314 (54680), 283 (50280).

[Ru(tpy-HImzphen)$_2$](ClO_4)$_2$·H_2O (3). A mixture of tpy-HImzphen (110 mg, 0.21 mmol) and $RuCl_3.3H_2O$ (36.5 mg, 0.1 mmol) in 25 mL of ethylene glycol was stirred under reflux at 180 °C for 18 h. The resulting deep red solution was cooled to room temperature and was then added into an aqueous solution of $NaClO_4·H_2O$ and stirred for 10 min, when a red microcrystalline compound deposited. The precipitate was filtered, washed several times with cold water, and then dried under vacuum. The compound was then purified by silica gel column chromatography using acetonitrile as the eluent. The eluents were reduced to small volume and to it was then added aqueous solution of $NaClO_4·H_2O$ when a red micro crystalline compound deposited. The precipitate was collected and washed several times with cold water. Further purification was carried out by recrystallization of the compound from a mixture of MeCN and MeOH (1:5) in the presence of a few drops of aqueous 10^{-4} M perchloric acid (78 mg, Yield: 58%). Anal. Calcd. for $C_{72}H_{48}N_{10}Cl_2O_9Ru$: C, 63.16; H, 3.53; N, 10.23. Found: C, 63.13; H, 3.56; N, 10.19. ^{1}H NMR data {300 MHz, DMSO-d_6, δ(ppm)}: 13.72 (s, 2H, NH imidazole), 9.62 (s, 4H, H3′), 9.18 (d, 4H, J = 8.2 Hz, H6), 8.92 (t, 4H, J = 9.6 Hz, H9), 8.74−8.63 (m, 12H, 4H7 + 4H8 + 4H12), 8.12 (t, 4H, J = 7.7 Hz, H4), 7.85−7.77 (m, 4H, H11), 7.74−7.67 (m, 4H, H10), 7.62 (d, 4H, J = 5.4 Hz, H3), 7.33 (t, 4H, J = 6.5 Hz, H5). ESI-MS (positive, CH_3CN) m/Z = 575.78 (100%) $[Ru(tpy\text{-}HImzphen)_2]^{2+}$. UV−vis [DMSO; λ_{max}, nm (ε, M^{-1} cm^{-1})]: 506 (60120), 381 (49520), 334 (69680), 316 (82560), 281 (92000).

[Os(tpy-HImzphen)$_2$](ClO_4)$_2$·2H_2O (4). A mixture of tpy-HImzphen (110 mg, 0.21 mmol) and K_2OsCl_6 (48.01 mg, 0.10 mmol) in 20 mL of degassed ethylene glycol was heated at 200 °C with continuous stirring for 24 h. The resulting black solution was cooled to room temperature and then poured into 10 mL aqueous solution of $NaClO_4·H_2O$ (1.0 g) and stirred for few minutes when a black precipitate appeared. The precipitate was collected by filtration and washed several times with water and then dried under vacuum. The crude product was purified by silica gel column chromatography eluting with acetonitrile. On recrystallization from acetonitrile-methanol (1:2) mixture in the presence of a few drops of aqueous 10^{-4} M perchloric acid afforded black crystals (80 mg, Yield: 56%). Anal. Calcd. for $C_{72}H_{50}N_{10}Cl_2O_{10}Os$: C, 58.57; H, 3.41; N, 9.49. Found: C, 58.55; H, 3.44; N, 9.46. ^{1}H NMR data {300 MHz, DMSO-d_6, δ(ppm)}: 13.73 (s, 2H, NH imidazole), 9.63 (s, 4H, H3′), 9.16 (d, 4H, J = 8.3 Hz, H6), 8.92 (d, 4H, J = 8.2 Hz, H9), 8.69−8.65 (m, 12H, 4H7 + 4H8 + 4H12), 7.98 (t, 4H, J = 7.6 Hz, H4), 7.81 (t, 4H, J = 7.4 Hz, H11), 7.71 (t, 4H, J = 7.3 Hz, H10), 7.50 (d, 4H, J = 5.6 Hz, H3), 7.26 (t, 4H, J = 6.5 Hz, H5). ESI-MS (positive, CH_3CN) m/Z = 621.22 (100%) $[Os(tpy\text{-}HImzphen)_2]^{2+}$. UV−vis [DMSO; λ_{max}, nm (ε, M^{-1} cm^{-1})]: 680 (12530), 650 (10680), 506 (60000), 398 (62910), 375 (65960), 322 (98930).

Physical Measurements. Elemental (C, H, and N) analyses were performed on a Perkin−Elmer 2400II analyzer. Electrospray ionization mass spectra (ESI−MS) were obtained on a Micromass Qtof YA 263 mass spectrometer. ^{1}H and {^{1}H−^{1}H} COSY spectra were obtained on a Bruker Avance DPX 300 spectrometer using DMSO−d_6 solutions. For a typical titration experiment, 3 μL aliquots of a tetrabutylammonium (TBA) salt of the anion (0.2 M in DMSO−d_6) were added to a DMSO−d_6 solution of the complexes (2.5×10^{-3} M).

Electronic absorption spectra were obtained with a Shimadzu UV 1800 spectrophotometer at room temperature. For a typical titration experiment, 2 μL aliquots of a TBA salts of F^-, Cl^-, Br^-, I^-, AcO^-, ClO_4^-, and $H_2PO_4^-$ ($\sim 4.0 \times 10^{-3}$ M) were added to a 2.5 mL solution of the complexes ($\sim 2.0 \times 10^{-5}$ M). The binding/equilibrium constants were evaluated from the absorbance data using eq 1.[28]

$$A_{obs} = (A_0 + A_\infty K[G]_T)/(1 + K[G]_T) \quad (1)$$

where A_{obs} is the observed absorbance, A_0 is the absorbance of the free receptor, A_∞ is the maximum absorbance induced by the presence of a given anionic guest, $[G]_T$ is the total concentration of the guest, and K is the binding constant of the host−guest entity. Binding constants were performed in duplicate, and the average value is reported.

Emission spectra were recorded on Perkin−Elmer LS55 fluorescence spectrophotometer. The room temperature spectra were obtained either in acetonitrile or in dimethylsulfoxide solutions, while the spectra at 77 K were recorded in 4:1 ethanol−methanol glass. Photoluminescence titrations were carried out with the same sets of solutions as were made with spectrophotometry. Quantum yields were determined by a relative method using $[Ru(bpy)_3]^{2+}$ as the standard. Time-correlated single-photon-counting (TCSPC) measurements were carried out for the luminescence decay of complexes. For TCSPC measurement, the photoexcitation was made at 440 nm using a picosecond diode laser (IBH Nanoled-07) in an IBH Fluorocube apparatus. The fluorescence decay data were collected on a Hamamatsu MCP photomultiplier (R3809) and were analyzed by using IBH DAS6 software.

The electrochemical measurements were carried out with a BAS 100B electrochemistry system. A three-electrode assembly comprising a Pt (for oxidation) or glassy carbon (for reduction) working electrode, Pt auxiliary electrode, and an aqueous Ag/AgCl reference electrode were used. The cyclic voltammetric (CV) and square wave voltammetric (SWV) measurements were carried out at 25 °C in acetonitrile-dimethylformamide (9:1) solution of the complex (ca. 1 mM), and the concentration of the supporting electrolyte tetraethylammonium perchlorate (TEAP) was maintained at 0.1 M. All of the potentials reported in this study were referenced against the Ag/AgCl electrode, which under the given experimental conditions gave a value of 0.36 V for the ferrocene/ferrocenium couple. For electrochemical titrations 25 μL aliquots of TBA salts of the anions (2.0×10^{-2} M in acetonitrile) were added to a 5 mL (1.0×10^{-3} M) solution of sensors **1**−**4** in acetonitrile-dimethylformamide (9:1) mixture.

Experimental uncertainties were as follows: absorption maxima, ± 2 nm; molar absorption coefficients, 10%; emission maxima, ± 5 nm; excited-state lifetimes, 10%; luminescence quantum yields, 20%; redox potentials, ± 10 mV.

X-ray Crystal Structure Determination. Single crystals of all the three compounds (**2**, **3**, and **4**) were obtained by diffusing toluene to the acetonitrile-dichloromethane (1:4) solution of the compounds. X-ray diffraction data for the crystals mounted on a glass fiber and coated with perfluoropolyether oil were collected on a Bruker-AXS SMART APEX II diffractometer at room temperature equipped with CCD detector using graphite-monochromated Mo Kα radiation (λ = 0.71073 Å). Crystallographic data and details of structure determination

Table 1. Crystallographic Data for $[2]^{2+}$, $[3]^{2+}$, and $[4]^{2+}$

	2	3	4
formula	$C_{55}H_{36}N_{10}Cl_2O_{10}Ru$	$C_{72}H_{46}N_{10}Cl_2O_9Ru$	$C_{72}H_{46}N_{10}Cl_2O_{10}Os$
fw	1168.91	1367.16	1472.29
T (K)	296(2)	293(2)	293(2)
cryst syst	triclinic	triclinic	triclinic
space group	$P\bar{1}$	$P\bar{1}$	$P\bar{1}$
a (Å)	13.161(3)	11.411(5)	11.442(5)
b (Å)	15.363(3)	17.197(5)	17.217(5)
c (Å)	16.558(4)	18.229(5)	18.199(5)
α (deg)	77.681(6)	106.168(5)	106.331(5)
β (deg)	83.095(6)	101.939(5)	102.036(5)
γ (deg)	69.194(6)	98.299(5)	98.161(5)
V (Å^3)	3053.9(11)	3282.8(19)	3287.1(19)
D_c (g cm^{-3})	1.271	1.383	1.488
Z	2	2	2
μ (mm^{-1})	0.404	0.386	2.089
F(000)	1188	1396	1476
θ range (deg)	1.44−24.79	1.20−25.10	1.21−25.09
data/restraints/params	10415/0/739	11581/0/842	11645/0/841
GOF on F^2	0.868	0.968	0.876
R1 $[I > 2\sigma(I)]^a$	0.0548	0.0584	0.0457
wR2 (all data)^b	0.1595	0.1702	0.1334
$\Delta\rho_{max}/\Delta\rho_{min}$ (e Å)	0.541/−0.512	0.692/−0.630	1.245/−0.909

^{a}R1(F) = $\sum||F_o| - |F_c||/\sum|F_o|$. ^{b}wR2 ($F^2$) = $[\sum w(F_o^2 - F_c^2)^2/\sum w(F_o^2)^2]^{1/2}$.

are summarized in Table 1. The data were processed with SAINT,[29] and absorption corrections were made with SADABS.[29] The structure was solved by direct and Fourier methods and refined by full-matrix least-squares based on F^2 using the WINGX software which utilizes SHELX-97.[30] For the structure solution and refinement the SHELXTL software package[31] was used. The nonhydrogen atoms were refined anisotropically, while the hydrogen atoms were placed with fixed thermal parameters at idealized positions. The electron density map also showed the presence of some unassignable peaks, which were removed by running the program SQUEEZE.[32]

CCDC reference numbers: 836472 for **2**, 836473 for **3**, and 836474 for **4**.

RESULTS AND DISCUSSION

Synthesis and Characterization. A mixture of 9,10-phenanthrenedione and 4′-(*p*-formylphenyl)-2,2′:6′,2″- terpyridine (tpy-PhCHO) in 1:1 molar ratio was subjected to undergo condensation under refluxing condition in acetic acid in presence of excess of ammonium acetate for the synthesis of the desired ligand, tpy-HImzphen. The homo- and heteroleptic complexes derived from the ligand are presented in Chart 1. For the synthesis of heteroleptic ruthenium(II) complex $[(tpy\text{-}PhCH_3)Ru(tpy\text{-}HImzphen)]^{2+}$ (**1**), the solvated cation $[(tpy\text{-}PhCH_3)Ru(acetone)_3]^{3+}$, generated by reacting stoichiometric amounts of $[(tpy\text{-}PhCH_3)RuCl_3]$ and $AgBF_4$ acts as a better precursor relative to $[(tpy\text{-}PhCH_3)RuCl_3]$ itself in terms of reaction time and yield. Thus, the reaction between tpy-HImzphen and $[(tpy\text{-}PhCH_3)Ru(acetone)_3]^{3+}$ in refluxing ethanol solution produces smoothly complex **1**. On the other hand, dehalogenation of the ruthenium(III) precursor, $[(H_2pbbzim)RuCl_3]$ with $AgBF_4$ in acetone is far less efficient. Thus, complex **2** has been straightforwardly prepared by reacting $[(H_2pbbzim)RuCl_3]$ with tpy-HImzphen in ethylene glycol in the temperature range 180−200 °C, followed by anion metathesis with $NaClO_4$. The homoleptic complexes **3** and **4** were synthesized directly by reaction of $RuCl_3{\cdot}3H_2O$ and K_2OsCl_6, respectively with 2 equiv of tpy-HImzphen in refluxing ethylene glycol solution, followed by chromatography and counteranion exchange with $NaClO_4$. Temperature was found to be a key factor for the synthesis of these metal complexes. The compounds were finally recrystallized from acetonitrile-methanol mixture under mildly acidic conditions to keep the imidazole NH protons intact. All the compounds have been characterized by their elemental (C, H, and N) analyses, ESI-MS, UV−vis, ^{1}H NMR spectroscopic measurements, and the results are given in the Experimental Section. The ESI mass spectra of the complexes and their simulated isotopic patters are shown in Figures S1 and S2 (Supporting Information).

Description of the Crystal Structure of the Complexes (2^{2+}, 3^{2+}, and 4^{2+}). ORTEP representations of the complex cations are shown in Figure 1, and selected bond distances and angles are given in Table 2. In each of the bis-chelated homoleptic ruthenium(II) and osmium(II) complexes **3** and **4**, the bivalent metal is coordinated by the tridentate ligand and has a distorted octahedral geometry having a meridional N_3N_3 chromophore. Both the complexes crystallized in the triclinic form with space group, $P\bar{1}$. The chelate bite angles span the range between 78.51(13) and 79.23(14)° for **3** and between 78.14(18) and 79.22(19)° for **4**. It is to be noted that although the interligand trans angle made by N4−Ru−N7 is 176.03(14)° and is very close to linearity, the intraligand trans angle N6−Ru−N8 is 157.65(13)°, and deviates significantly from linearity. The ruthenium−nitrogen bond lengths are within 1.975(3)−2.067(3) Å, whereas the osmium−nitrogen bond lengths lie between 1.978(4) and 2.071(5) Å. Similar Ru−N and Os−N bond distances have been previously observed in Ru(II) and Os(II) terpyridine type complexes.[7,13,22a] The central Ru−N bond length 1.975(3) Å is shorter than the two outer bonds, 2.051(4) and 2.067(3) Å, to each ligand probably because of efficient overlap of the metal t_{2g} orbital with the π^* orbitals of the central pyridyl ring. The dihedral angles between the central pyridine plane and the two lateral ones are different on each side of the metal center, and they vary between 5.42° and

dx.doi.org/10.1021/ic201610w | Inorg. Chem. 2011, 50, 12586−12600

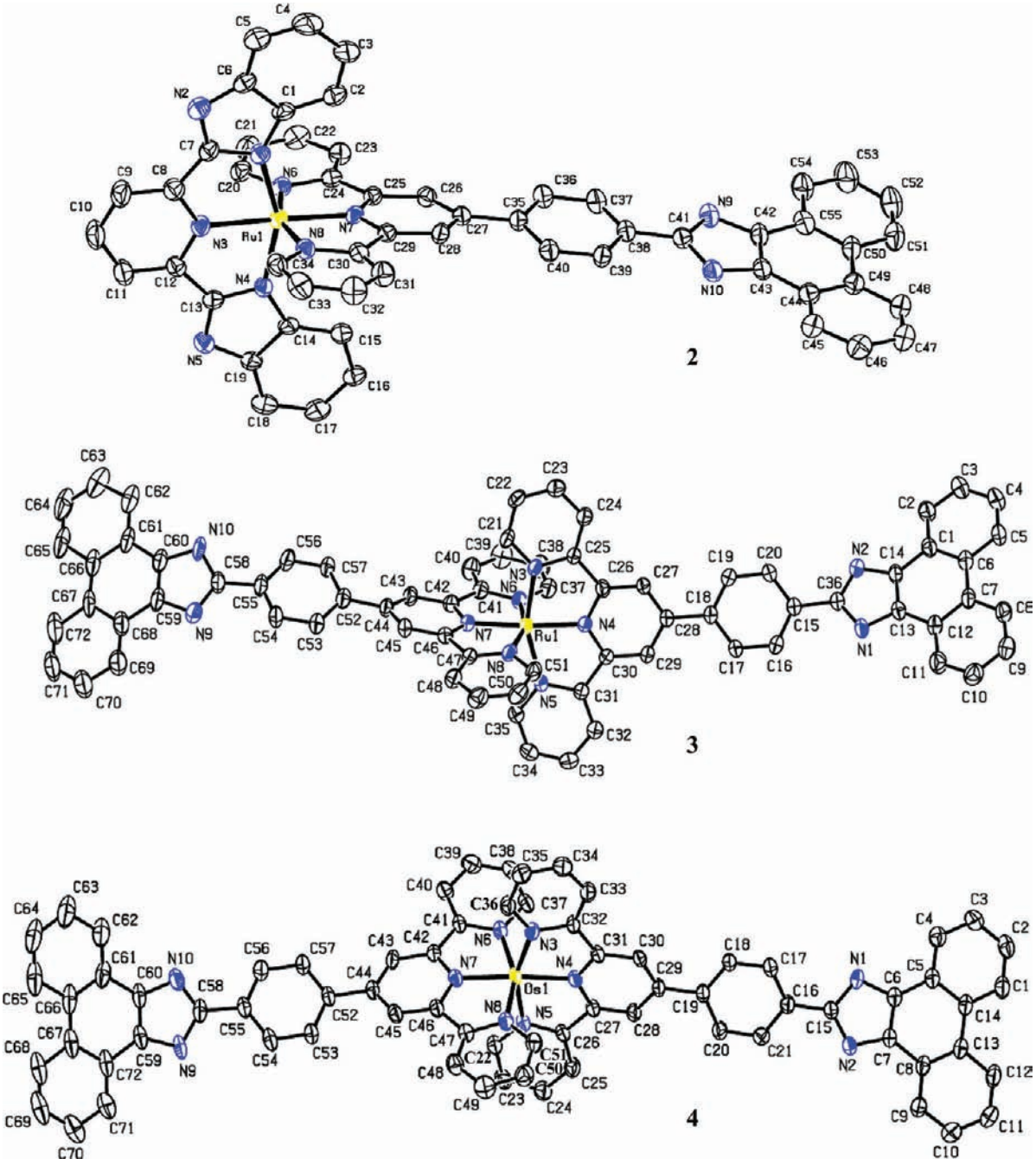

Figure 1. ORTEP representations of 2^{2+}, 3^{2+}, and 4^{2+} showing 30% probability of thermal ellipsoid. Hydrogen atoms are omitted for clarity.

12.72° for **3** and between 4.81° and 12.72° for **4**, while the dihedral angle between the central pyridine and phenyl ring of tpy-HImzphen is 24.67° and 26.71° for **3** and 23.73° and 25.18° for **4**. Again the phenanthrene-imidazole moiety, which is almost coplanar, is twisted from the plane of the phenyl group, and the dihedral angles lie in the range of 23.52°–25.75°.

The heteroleptic complex $[(H_2pbbzim)Ru(tpy\text{-}HImzphen)]^{2+}$ (**2**) also crystallized in a triclinic unit cell of the $P\bar{1}$ space group (Figure 1). The structure displays the expected geometry, with both ligands coordinated in tridentate, meridional fashion to the ruthenium(II) center. In contrast to the homoleptic complexes, the dihedral angles between central pyridine and the phenyl as well as between phenyl and phenanthreneimidazole moiety of heteroleptic complex **2** are small. The ruthenium–nitrogen bond lengths in tpy-HImzphen are within 1.966(3)–2.054(4) Å, whereas in H_2pbbzim are relatively longer, 2.016(3)–2.069(4) Å. Overall, only small differences in the coordination geometry have been detected when a tpy ligand is replaced by H_2pbbzim or tpy-HImzphen.

Proton NMR Spectra. ^{1}H NMR spectra of complexes **1**–**4** have been recorded in DMSO-d_6, and their chemical shift values are given in the Experimental Section. Figure 2 shows the ^{1}H NMR spectra of the complexes **1**–**4**. The assignments made for the observed chemical shifts, according to the numbering scheme (shown in Scheme 1), are listed in Table S1 (Supporting Information). The spectral assignments of the complexes have been made with the help of their {^{1}H–^{1}H}

dx.doi.org/10.1021/ic201610w | *Inorg. Chem.* 2011, 50, 12586–12600

Table 2. Selected Bond Distances (Å) and Angles (deg) for $[2]^{2+}$, $[3]^{2+}$, and $[4]^{2+}$

2		3		4	
Ru−N(1)	2.069(4)	Ru−N(3)	2.061 (3)	Os−N(3)	2.069(4)
Ru−N(3)	2.016(3)	Ru−N(4)	1.977(3)	Os−N(4)	1.979(4)
Ru−N(4)	2.066(4)	Ru−N(5)	2.064(3)	Os−N(5)	2.071(5)
Ru−N(6)	2.049(4)	Ru−N(6)	2.067(3)	Os−N(6)	2.054(5)
Ru−N(7)	1.966(3)	Ru−N(7)	1.975(3)	Os−N(7)	1.978(4)
Ru−N(8)	2.054(4)	Ru−N(8)	2.051(4)	Os−N(8)	2.054(5)
N(1)−Ru−N(3)	78.03(14)	N(3)−Ru−N(4)	79.17(13)	N(3)−Os−N(4)	78.34(17)
N(1)−Ru−N(4)	155.78(14)	N(3)−Ru−N(5)	157.68(13)	N(3)−Os−N(5)	157.21(18)
N(1)−Ru−N(6)	92.43(14)	N(3)−Ru−N(6)	98.19(13)	N(3)−Os−N(6)	87.16(18)
N(1)−Ru−N(7)	103.75(13)	N(3)−Ru−N(7)	97.12(13)	N(3)−Os−N(7)	106.17(18)
N(1)−Ru−N(8)	92.05(14)	N(3)−Ru−N(8)	86.97(13)	N(3)−Os−N(8)	96.95(19)
N(3)−Ru−N(4)	77.74(13)	N(4)−Ru−N(5)	78.51(13)	N(4)−Os−N(5)	78.87(17)
N(3)−Ru−N(6)	101.75(14)	N(4)−Ru−N(6)	103.28(13)	N(4)−Os−N(6)	103.92(18)
N(3)−Ru−N(7)	178.13(14)	N(4)−Ru−N(7)	176.03(14)	N(4)−Os−N(7)	175.22(16)
N(3)−Ru−N(8)	100.11(14)	N(4)−Ru−N(8)	99.04(13)	N(4)−Os−N(8)	98.83(18)
N(4)−Ru−N(6)	92.35(13)	N(5)−Ru−N(6)	87.07(13)	N(5)−Os−N(6)	98.45(18)
N(4)−Ru−N(7)	100.48(13)	N(5)−Ru−N(7)	105.18(13)	N(5)−Os−N(7)	96.61(18)
N(4)−Ru−N(8)	92.29(14)	N(5)−Ru−N(8)	96.39(13)	N(5)−Os−N(8)	86.41(18)
N(6)−Ru−N(7)	78.84(13)	N(6)−Ru−N(7)	78.56(14)	N(6)−Os−N(7)	78.14(18)
N(6)−Ru−N(8)	158.14(13)	N(6)−Ru−N(8)	157.65(13)	N(6)−Os−N(8)	157.24(19)
N(7)−Ru−N(8)	79.31(13)	N(7)−Ru−N(8)	79.23(14)	N(7)−Os−N(8)	79.22(19)

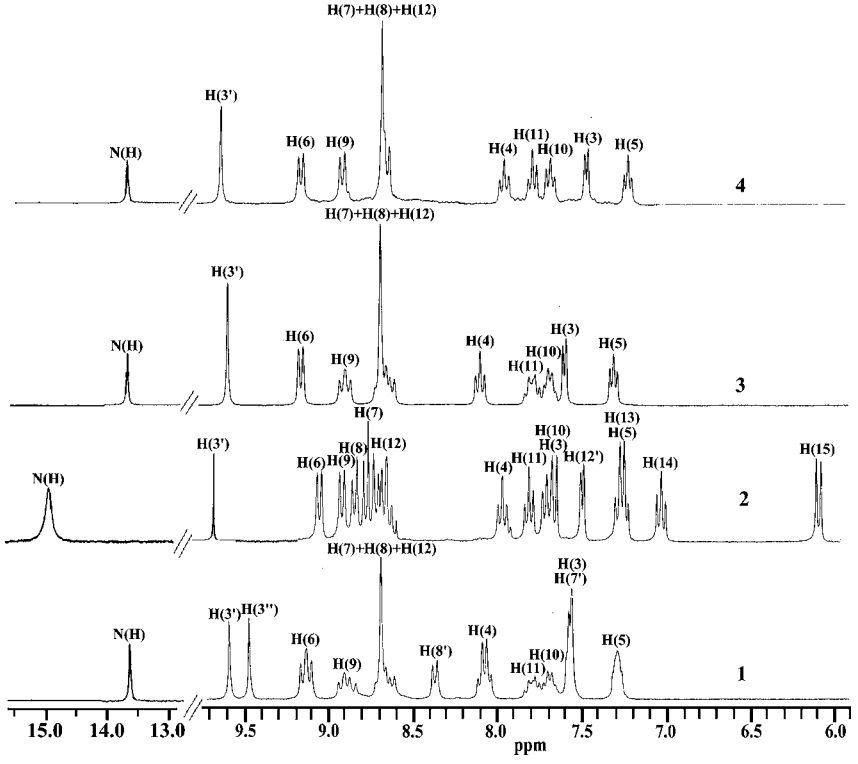

Figure 2. ^{1}H NMR spectra of **1**−**4** in DMSO-d_6. Atoms numbering for the complexes are shown in Scheme 1.

COSY spectra (Figure S3, Supporting Information), relative areas of the peaks, and taking into consideration the usual ranges of J values for H_2pbbzim and 4′-substituted tpy derivatives.[7−14,22]

Absorption Spectra. The UV−vis spectra of the complexes **1**−**4** are shown in Figure 3, and their absorption maxima and molar extinction coefficients (ε) are presented in Table 3, which also contains data for model complexes. The absorption spectra of the complexes are basically of similar type exhibiting a number of bands in the UV−vis region. Assignments were made by comparison to $[M(tpy)_2]^{2+}$ and related M(II) monotpy (M = Ru^{II} and Os^{II}) type complexes.[1,2,4] Thus, two very intense bands observed around 280 and 315 nm (ε = 50000−100000 M^{-1} cm^{-1}) in the complexes are due to $\pi-\pi^*$ ligand centered transitions, while the next higher wavelength absorptions occurring between 350 and 390 nm are due to internal transitions of the ligands. All the complexes exhibit a strong absorption peak in the range of 492−506 nm

dx.doi.org/10.1021/ic201610w | Inorg. Chem. 2011, 50, 12586−12600

Scheme 1

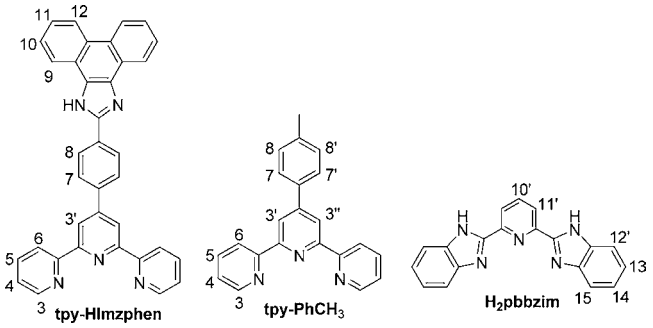

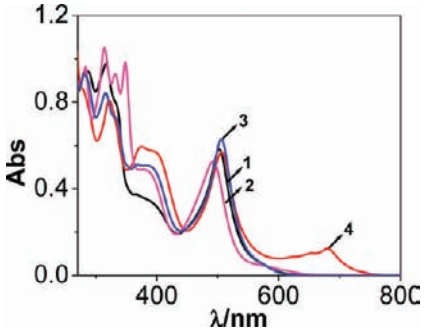

Figure 3. Absorption spectra of **1**, **3**, and **4** in dimethylsulfoxide and **2** in acetonitrile at room temperature.

(ε = 27000−60000 M^{-1} cm^{-1}) which can be attributed to $^1[M^{II}(d\pi)^6] \rightarrow {}^1[M^{II}(d\pi)^5$tpy-HImzphen$(\pi^*)^1]$ charge transfer (^{1}MLCT) transition. Absorption spectrum of **2** also contains a low-energy shoulder at ∼580 nm. This band probably arises from $^1[Ru^{II}(d\pi)^6] \rightarrow {}^3[Ru^{II}(d\pi)^5$tpy-HImzphen$(\pi^*)^1]$ transitions which are allowed because of spin−orbit coupling which has the effect of mixing excited singlet and triplet states.[33] Analysis of the spectrum of **2** shows that the energy difference between the lowest, intense singlet, $^1[Ru^{II}(d\pi)^6] \rightarrow {}^1[Ru^{II}(d\pi)^5$tpy-HImzphen$(\pi^*)^1]$ band at 492 nm (20325 cm^{-1}, ε = 27280 M^{-1} cm^{-1}) and the triplet $^1[Ru^{II}(d\pi)^6] \rightarrow {}^3[Ru^{II}(d\pi)^5$tpy-HImzphen$(\pi^*)^1]$ band at ∼580 nm (∼ 17241 cm^{-1}, ε = 1980 M^{-1} cm^{-1}) is 3084 cm^{-1}, which is of similar magnitude to the singlet−triplet splitting energy for $[Ru(tpy)_2]^{2+}$ and the other monotpy complexes.[1,4,33] The osmium(II) compound, **4** additionally exhibits intense well-defined broad bands around 650 and 680 nm (ε = 12500 M^{-1} cm^{-1}) which again arise because of a spin forbidden ^{3}MLCT transition that directly populates the triplet MLCT state. In the case of Os^{II}, as the extent of spin−orbit coupling is greater than that of Ru^{II}, the intensity of the spin forbidden ^{3}MLCT transition in **4** is much higher compared to **2**. It is of interest to note that the lowest energy ^{1}MLCT absorption band for the Ru(II) and Os(II) complexes (**1**−**4**) is shifted to lower energy compared to the parent $[Ru(tpy)_2]^{2+}$ (474 nm) and $[Os(tpy)_2]^{2+}$ (477 nm) complexes.[1d] Again, the MLCT absorption of $[Ru(H_2pbbzim)_2]^{2+}$ was observed at 475 nm, which is almost

Table 3. Spectroscopic and Photophysical Data of 1, 3, and 4 in Dimethylsulfoxide and 2 in Acetonitrile Solutions

		luminescence						
		at 298 K[a]					at 77 K[b]	
complexes	absorption λ_{max}, nm (ε, M^{-1} cm^{-1})	λ_{max} nm	τ, ns	Φ (×10^{-3})	k_r, s^{-1} (×10^5)	k_{nr}, s^{-1} (×10^7)	λ_{max} nm	Φ
1	502(37350)	668	10.2	1.27	1.25	9.79	641	0.25
	390(27760)							
	316(71000)							
	285(73700)							
2	492(27280)	681	55.5	3.26	0.81	1.79	675	0.22
	382(24810)							
	348(51790)							
	314(54680)							
	283(50280)							
3	505(60120)	667	15.8	1.9	1.20	6.32	644	0.17
	381(49520)							
	334(69680)							
	316(82560)							
	281(92000)							
4	680(12530)	760	30.2	58.2	19.3	3.29	730	0.12
	650(10680)							
	506(60000)							
	398(62910)							
	375(65960)							
	322(98930)							
5[c]	474(10400)	629	0.25	≤0.05	0.04	90.9	598	
6[d]	490(28000)	640	<5.0	≤0.03			628, 681(sh)	
7[e]	475(17400)							
8[f]	657(3650)	718	269	14.0			689	0.124
	477(13750)							
9[g]	667(6600)	734	220	21.0			740	0.049
	490(26000)							

[a]In DMSO (1,3 and 4) and CH_3CN (2). [b]MeOH-EtOH(1:4) glass. [c]$[Ru(tpy)_2]^{2+}$.[1d] [d]$[Ru(tpy\text{-}PhCH_3)_2]^{2+}$.[1d] [e]$[Ru(H_2pbbzim)_2]^{2+}$.[34a] [f]$[Os(tpy)_2]^{2+}$.[1d] [g]$[Os(tpy\text{-}PhCH_3)_2]^{2+}$.[1d]

dx.doi.org/10.1021/ic201610w | Inorg. Chem. 2011, 50, 12586−12600

comparable in energy to that of $[Ru(tpy)_2]^{2+}$.[34] The differences in the MLCT bands between parent $[M(tpy)_2]^{2+}$ (M = Ru^{II} and Os^{II}) and the complexes **1**−**4** reflect the energy differences of the π^* orbitals of the individual ligands. It is interesting to note that the complexes under investigation have very high molar absorptivities in the visible region compared to the parent $[M(tpy)_2]^{2+}$ (M = Ru^{II} and Os^{II}) complexes, which make them good candidate for light-harvesting materials. It may also be noted that the molar extinction coefficients (ε) of the ^{1}MLCT band in the homoleptic Ru(II) complex (**3**) is much higher than those for the heteroleptic analogues (**1** and **2**), which probably arises because of extensive delocalization of tpy-HImzphen.

Luminescence Spectra. The emission spectral behavior of complexes **1**−**4** have been studied at room temperature in either acetonitrile or dimethylsulfoxide and at 77 K using ethanol−methanol (4:1) glass. Table 3 also summarizes the emission maxima, quantum yield (Φ), and lifetime (τ) of the complexes together with the data available for the reference mononuclear compounds. All the three ruthenium(II) complexes on excitation at their MLCT absorption maximum exhibit one broad luminescent band, which lies between 667 (**3**) and 681 nm (**2**) at 300 K and between 641 (**1**) and 675 nm (**2**) at 77 K (Figure 4) depending upon the coligands other

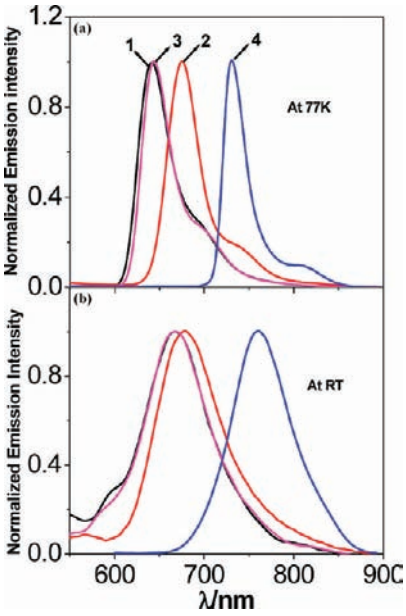

Figure 4. Photoluminescence spectra of **1**, **3**, and **4** in dimethylsulfoxide and of **2** in acetonitrile at room temperature (a) and at 77 K in ethanol−methanol (4:1) glass (b).

than tpy-HImzphen. The excitation of **4** into the MLCT peak at 500 nm also resulted in the appearance of a luminescence band centered at 760 nm at 300 K and 730 nm at 77 K. On the basis of extensive investigations performed on $[M(tpy)_2]^{2+}$ (M = Ru^{II} and Os^{II}) and related complexes, it can be concluded that the bands have the characteristics of emission from the ^{3}MLCT excited state, which corresponds to a spin-forbidden $M^{II}(d\pi) \rightarrow$ tpy-HImzphen(π^*) transition.[1,2,4] In line with absorption spectral data, the emission maximum of the complexes (**1**−**4**) is also shifted to lower energy compared to the ^{3}MLCT emission of the parent $[Ru(tpy)_2]^{2+}$ (629 nm) and $[Os(tpy)_2]^{2+}$ (718 nm) complexes.[1d] The most striking feature of this class of ruthenium(II) compounds is that they are luminescent at room temperature in fluid solutions though the parent $[Ru(tpy/tpy\text{-}PhCH_3)_2]^{2+}$[5] or $[Ru(H_2pbbzim)_2]^{2+}$ [34a] are non−luminescent. The room-temperature lifetimes of the complexes which lie between 10 (**1**) and 55 ns (**2**), are significantly greater than that of parent $Ru(tpy)_2$ (0.25 ns) (Figure S4, Supporting Information). It should be noted that the enhanced luminescence properties of the complexes have been achieved without lowering the excited-state energy significantly. On going from fluid solution to frozen glass, the emission maxima get blue−shifted with a significant increase of emission intensity and quantum yield, typical of the ^{3}MLCT emitters.[1,2] The zero−zero excitation energy (E_{00}) values of the ^{3}MLCT excited states of the complexes (**1**−**4**) were estimated from the energies at the intersection point of the absorption and emission band of the complexes. The E_{00} values thus estimated are 2.17 eV for $[(tpy\text{-}PhCH_3)Ru(tpy\text{-}HImzphen)]^{2+}$ (**1**), 2.10 eV for $[(H_2pbbzim)Ru(tpy\text{-}HImzphen)]^{2+}$ (**2**), 2.18 eV for $[Ru(tpy\text{-}HImzphen)_2]^{2+}$ (**3**), and 1.79 eV for $[Os(tpy\text{-}HImzphen)_2]^{2+}$ (**4**). At 77 K, each spectrum displays a well-defined vibronic progression in the lower energy region with spacing of ∼1315 cm^{-1} for **1**, ∼1303 cm^{-1} for **2**, ∼1356 cm^{-1} for **3**, and ∼1353 cm^{-1} for **4**, which are similar to those reported for $[M(tpy)_2]^{2+}$ (M = Ru^{II} and Os^{II}), the other monotpy complexes of Ru(II) and Os(II), and can be attributed to aromatic stretching vibrations of the ligands.[33,35]

The excited-state lifetimes of Ru(II) polypyridine complexes are governed by the nonradiative decay rate constant k_{nr}, given by eq 2[1,7]

$$k_{nr} = k_{nr}^{0} + k'_{nr} \quad (2)$$

The overall radiationless decay is the sum of two terms. The first one, k_{nr}^0, is directly related to the energy transfer from the MLCT state to the ground state, whereas the second term, k'_{nr}, is related to the thermally activated process that takes into account a surface-crossing from the lowest-lying MLCT state to a closely lying metal-centered (MC) level and therefore depends upon the energy gap ΔE between MLCT and MC states.[1,2,4] For Ru(II) complexes with tridentate ligands, the second term normally dominates the equation.[4,7] The small ΔE between MLCT and MC states in Ru(II) tridentate polypyridine complexes, a consequence of the reduced ligand field strength experienced by the metal center compared to Ru(II) bidentate polypyridine ligands, is due to an ill-fitted octahedral arrangement, which in turn is responsible for the poor room-temperature luminescence properties of $Ru(tpy)_2$-type complexes.[1,2,4] On the other hand, for the related osmium(II) complex this deactivation channel is unimportant because osmium(II) exhibits a considerably stronger ligand field than ruthenium(II), so that ^{3}MLCT → ^{3}LF crossing should remain inaccessible even at room temperature. Moreover, as the osmium system $[Os(tpy\text{-}HImzphen)_2]^{2+}$ (**4**), does not possess this low-lying LF state, hence deactivation is only from the ^{3}MLCT state leading to the observed longer excited state lifetime compared to its analogous Ru(II) compound. In the present systems under investigation, the energy of the MC level being considered to be constant, the MLCT emitting level is decreased in energy by modulating the electronic influence of the terpyridine moiety by extensive delocalization due to the phenanthrene-imidazole group, thereby reducing the efficiency of the MLCT-to-MC surface-crossing pathway. However, the larger energy gap between MLCT and MC states may not be the only reason to fully justify the relatively long luminescence lifetimes of the complexes.

Solvent Effect. It is interesting to note that the lowest energy absorption maxima of the complexes are strongly influenced by the solvents. The solvent effect is particularly

dx.doi.org/10.1021/ic201610w | Inorg. Chem. 2011, 50, 12586−12600

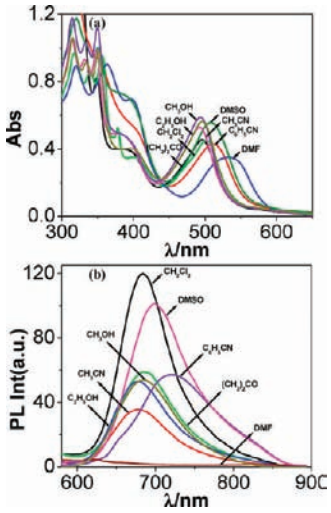

Figure 5. (a) Absorption and (b) photoluminescence spectra of **2** in different solvents.

Table 4. Absorption and Luminescence Spectral Data of 2 in Different Solvents

solvents	λ_{max}, nm (ε, M^{-1} cm^{-1})	λ_{emi}, nm Φ ($\times 10^{-3}$)
CH_2Cl_2	502(23380)	684,
	403(18060)	9.74
	378(27050)	
	356(49290)	
	340(44500)	
	317(49970)	
CH_3OH	494(30750)	685,
	390(22750)	4.22
	350(53260)	
	333(50230)	
	315(57430)	
$(CH_3)_2CO$	496(24590)	688,
	393(21360)	5.37
	349(44450)	
C_2H_5OH	496(29000)	678,
	390(24300)	4.72
	351(50000)	
	334(47400)	
	315(55560)	
CH_3CN	492(28520)	681,
	384(26230)	3.26
	348(53240)	
	332(50410)	
	314(56900)	
DMF	533(19880)	
	397(39480)	
	363(51220)	
	320(50760)	
DMSO	508(31600)	700,
	385(41160)	8.60
	350(56900)	
	320(66720)	
C_6H_5CN	511(22160)	722,
		7.04

dramatic for **2**. Figure 5a shows the absorption spectra for **2** in different solvents. From Table 4, it is seen that the MLCT band maxima shift to longer wavelength with the increase in polarity as well as with the extent of hydrogen bonding ability of the solvent. For instance, the lowest energy MLCT maxima in **2** shifted from 492 nm in CH_3CN to 533 nm in DMF ($\Delta\lambda_{max}$ = 41 nm) with concomitant change of color from yellow-orange to orange-brown. For the homoleptic complex **3**, the corresponding change is small, namely, 10 nm (498 to 508 nm) (Figure S5a, Supporting Information).

Figure 5b shows the emission spectra of **2** in different solvents. As compared with the absorption spectra, its emission spectral behavior shows significantly larger solvatochromism. By changing the solvents, the lowest energy emission maxima get red-shifted from 678 (C_2H_5OH) to 722 nm (C_6H_5CN) ($\Delta\lambda_{em}$ = 44 nm). In case of **3**, the corresponding change of the emission maxima is 13 nm (655 to 668 nm) (Figure S5b, Supporting Information). It is of interest to note that the emission intensity of **2** is quenched to a significant extent with DMF.

Redox Properties. The redox activities of complexes have been studied in acetonitrile solution, and the relevant electrochemical results are gathered in Table 5, together with

Table 5. Electrochemical Data[a] for 1−4 in Acetonitrile

compd	oxidation[b] $E_{1/2}$(ox), V	reduction[c] $E_{1/2}$(red), V
1	1.16	−1.17, −1.37, −1.74
2	1.11	−1.16, −1.45, −1.90
3	1.18	−1.17, −1.42, −1.74
4	0.90	−1.16, −1.42, −1.75
5[d]	1.30	−1.29, −1.54
6[e]	1.25	−1.24, −1.46
7[f]	0.76	−1.40, −1.70
8[g]	0.97	−1.25, −1.57
9[h]	0.93	−1.23, −1.54

[a]All the potentials are referenced against a Ag/AgCl electrode with $E_{1/2}$ = 0.36 V for the Fc/Fc^+ couple. [b]Reversible electron transfer process with a Pt working electrode. [c]$E_{1/2}$ values obtained from square wave voltammetric (SWV) using glassy carbon electrode. [d][Ru(tpy)$_2$]$^{2+}$.[1d] [e][Ru(tpy-PhCH$_3$)$_2$]$^{2+}$.[1d] [f][Ru(H$_2$pbbzim)$_2$]$^{2+}$.[34a] [g][Os(tpy)$_2$]$^{2+}$.[1d] [h][Os(tpy-PhCH$_3$)$_2$]$^{2+}$.[1d]

the results available for the reference mononuclear species. The complexes are found to undergo one reversible one-electron oxidation in the positive potential window (0 to +1.5 V) and three successive quasi-reversible reductions in the negative potential window (0 to −2.2 V) (Figure 6 and Figure S6, Supporting Information). In ruthenium(II) and osmium(II) polypyridyl complexes the highest occupied molecular orbital (HOMO) will be based on the metal center, and oxidative processes are therefore metal based, whereas the lowest unoccupied molecular orbital (LUMO) are ligand based and the reduction processes are ligand centered, in agreement with literature data and the reversibility of most of the processes.[1,2,36] Thus, the oxidation in the positive potential window has been assigned as a M^{II}/M^{III} (M = Ru and Os) oxidation process. The osmium(II) complex (**4**) showed (Figure 6) a notable cathodic shift in the potential for oxidation versus that of the Ru^{II} counterpart, which is attributed to the lowered intrinsic potential of the Os^{II} metal. The metal based oxidation potential of the complexes are significantly lower than that observed for $[M(tpy)_2]^{2+}$ (M = Ru and Os).[1d] This is in agreement with the spectroscopic data already noted in the previous sections and can be explained by the extensive delocalization of tpy-HImzphen ligand. In **4**, an irreversible

dx.doi.org/10.1021/ic201610w | Inorg. Chem. 2011, 50, 12586−12600

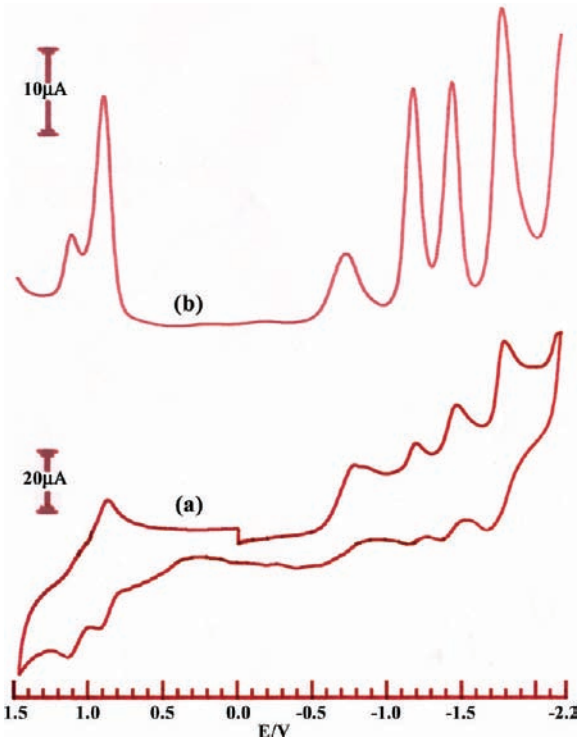

Figure 6. Cyclic (a) and square wave (b) voltammograms of **4** in acetonitrile showing both oxidation and reduction.

oxidation is also seen at 1.2 V which is probably due to a ligand-centered oxidation process. The first reduction process observed at about −1.16 V for all the complexes can be assigned as being tpy-HImzphen centered by comparing the reduction potentials of other tpy-based ruthenium(II) and osmium(II) complexes. In the homoleptic complexes (**3** and **4**) the second reduction occurs at the same potential (−1.42 V), while the second reduction in mixed ligand complexes occurs at −1.37 V for $[(\text{tpy-PhCH}_3)\text{Ru}(\text{tpy-HImzphen})]^{2+}$ (**1**) and −1.45 V for $[(\text{H}_2\text{pbbzim})\text{Ru}(\text{tpy-HImzphen})]^{2+}$ (**2**) being assigned as $\text{tpy-PhCH}_3/\text{tpy-PhCH}_3^-$ and $\text{H}_2\text{pbbzim}/\text{H}_2\text{pbbzim}^-$ ligand-centered processes, respectively. It is of interest to note that both the first and the second reduction potentials in the homoleptic complexes (**3** and **4**) appear to be insensitive to the nature of the coordinated metal leading to the conclusion that the reductions are largely ligand localized.[36]

■ ANION SENSING STUDIES OF THE METALLORECEPTORS

Colorimetric Signaling. The anion sensing abilities of the receptors **1**−**4** have been studied on a qualitative basis by visual examination of the anion-induced color changes in acetonitrile (**2**) and DMSO (**1**, **3**, and **4**) solutions (2×10^{-5} M) before and after the addition the anions as their TBA salts. The photograph in Figure 7 shows the dramatic color changes of the metalloreceptors as a result of adding 10 equiv of various anions such as F^-, Cl^-, Br^-, I^-, AcO^-, ClO_4^-, and $H_2PO_4^-$. Specifically, complexes **1**, **3**, and **4** are sensor selective for F^- only, whereas the complex **2** is the sensor for F^-, AcO^-, and to a lesser extent for $H_2PO_4^-$. The dramatic anion-specific response makes the complexes especially effective colorimetric anion sensors.

Absorption Signaling. UV−vis spectroscopy was employed to quantify the anion-induced spectral changes in **1**−**4**. As

Figure 7. Color changes that occur when the solutions of **1**−**4** are treated with various anions as their tetrabutylammonium (TBA) salts.

shown in Figure S7 (Supporting Information) and Figure 8, the position of the MLCT bands at 502, 505, and 506 nm for

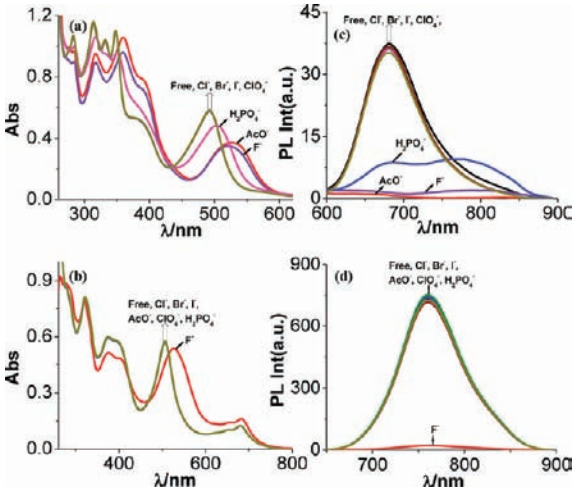

Figure 8. Changes in absorption (a, b) and luminescence (c, d) spectra of **2** in acetonitrile and **4** in dimethylsulfoxide solution upon the addition of different anions as their TBA salts.

complexes **1**, **3**, and **4**, respectively remain practically unchanged upon addition of 10 equiv of Cl^-, Br^-, I^-, AcO^-, ClO_4^-, and $H_2PO_4^-$ ions to their solutions (2.0×10^{-5} M) in DMSO. On the other hand, following the addition of 10 equiv of F^-, the said bands get red-shifted to 528, 533, and 527 nm, respectively, indicating that strong interactions occur between

dx.doi.org/10.1021/ic201610w | Inorg. Chem. 2011, 50, 12586−12600

the receptors and the anion. Compared to **1**, **3**, and **4**, receptor **2** in acetonitrile showed marked difference in sensing behavior as it has two different kinds of imidazole NH protons with different chemical environments. In case of **2**, as shown in Figure 8a, following the addition of 10 equiv of F^- and AcO^-, the MLCT band at 492 nm gets red-shifted to 527 nm. On addition of $H_2PO_4^-$ though the MLCT bands of **2** initially shifted to 505 nm, but addition of excess of $H_2PO_4^-$ leads to the precipitation of the resulting complex. On the other hand, the MLCT peak at 492 nm remains practically unchanged upon addition of 10 equiv of Cl^-, Br^-, I^-, and ClO_4^- ions to the solutions of **2**. These observations are in consonance with the visual changes already noted in Figure 7. The red-shift of the MLCT bands can be attributed to the second-sphere donor-acceptor interactions between metal coordinated terpyridyl-imidazole and the anions. Anion-induced deprotonation of the NH proton(s) in the complexes increase the electron density at the metal center leading to lowering of the MLCT band energies.

To get quantitative insight into sensor-anion interaction, spectrophotometric titrations of the receptors have been carried out with various anions. Figure 9a shows that with the

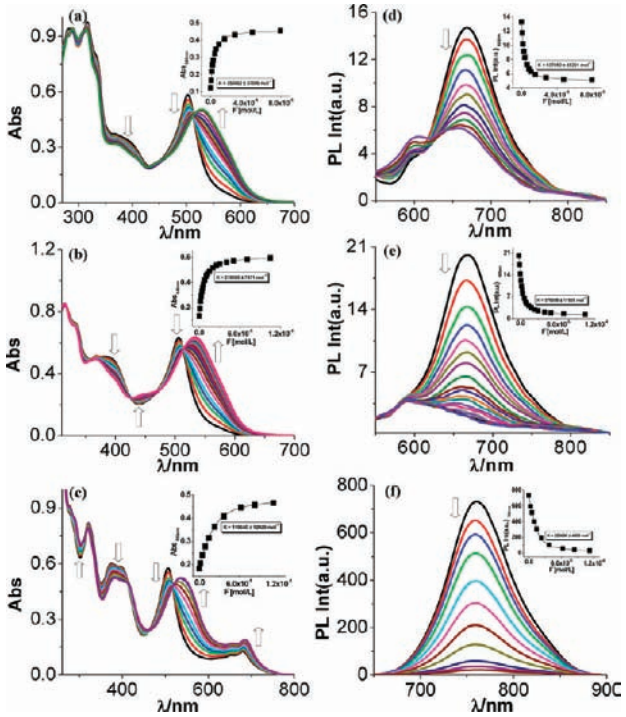

Figure 9. Changes in absorption (a–c) and photoluminescence (d–f) spectra of **1**, **3**, and **4** in dimethylsulfoxide solution upon the addition of F^- ion. The inset shows the fit of the experimental absorbance and luminescence data to a 1:1 binding profile.

incremental addition of TBAF to **1**, the MLCT band in the successive absorption curves undergo gradual red shifts during which they pass through the isosbestic point at 513 nm, while in the case of **3** (Figure 9b) such changes occur through three isosbestic points at 514, 470, and 425 nm. Similar trends of spectral changes have been observed for **4** as a function of F^- (Figure 9c). As the F^- ion is added to a solution of **4**, the MLCT absorption maxima at 506 nm get shifted to longer wavelength, 527 nm, with the concurrent development of four isosbestic points at 518, 463, 413, and 315 nm upon the addition of 10 equiv of F^-. In contrast, addition of the other anions to a DMSO solution of **1**, **3**, and **4** do not induce any change, indicating the inability of these anions to deprotonate the imidazole NH protons of the metalloreceptors. It is of interest to see the spectral changes for $[(H_2pbbzim)Ru(tpy\text{-}HImzphen)]$ $(ClO_4)_2$ (**2**) as it has a more complicated structure in respect of having different types of NH protons with different chemical environments compared to the other receptors under investigation. The spectral changes that occur for **2** as a function of AcO^- are shown in Figure 10. On close

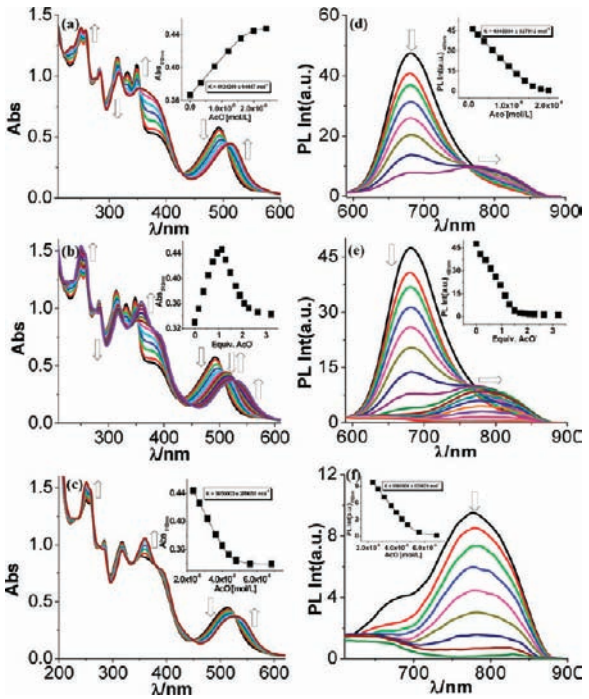

Figure 10. Changes in absorption (a–c) and photoluminescence (d–f) spectra of **2** in acetonitrile solution upon the addition of AcO^- ion. The inset shows the fit of the experimental absorbance and luminescence data to a 1:1 binding profile.

inspection of the changes in the spectral profiles with the incremental addition of anion, the occurrence of two successive reaction equilibria become evident. In the first case, spectral saturation occurs with the addition of 1 equiv of either F^- or AcO^- (shown in inset of Figure S8, Supporting Information and Figure 10), suggesting 1:1 receptor–anion interaction, while for the attainment of the second equilibrium process an excess of anions is required. The spectral patterns of **2** toward $H_2PO_4^-$ ion is almost the same with that of either F^- or AcO^- up to 1 equiv with 7 sharp isosbestic points at 505, 436, 353, 289, 273, 263, and 238 nm respectively (Figure S9, Supporting Information). On further addition of $H_2PO_4^-$ beyond 1 equiv, no noticeable changes in the spectral profile occurs and finally give rise to the precipitation of the resulting complex. It may be mentioned that in case of **2**, two successive deprotonation steps occur with a relatively lesser amount of both F^- and AcO^- compared with the other receptors where only one deprotonation step occurs at higher concentrations of F^- only as evidenced by spectrophotometric studies. The results indicate that the NH protons associated to H_2pbbzim moiety are successively deprotonated in case of **2** compared with **1**, **3**, and **4** where deprotonation occur from the tpy-HImzphen unit.

dx.doi.org/10.1021/ic201610w | *Inorg. Chem.* 2011, 50, 12586–12600

Table 6. Equilibrium/Binding Constants[a,b] (K, M^{-1}) for 1, 3, and 4 in Dimethylsulfoxide and for 2 in Acetonitrile Towards Various Anions at 298 K[c]

	1	2		3	4
anions	K	K_1	K_2	K	K
		from absorption spectra			
F^-	3.58×10^5	4.61×10^6	5.38×10^6	2.18×10^5	1.19×10^5
AcO^-	NA	4.12×10^6	5.95×10^6	NA	NA
$H_2PO_4^-$	NA	NA	NA	NA	NA
HO^-	3.88×10^5	7.11×10^6	6.99×10^6	5.15×10^5	4.55×10^5
		from emission spectra			
F^-	5.37×10^5	4.62×10^6	5.49×10^6	3.75×10^5	2.53×10^5
AcO^-	NA	4.04×10^6	5.96×10^6	NA	NA
$H_2PO_4^-$	NA	NA	NA	NA	NA
HO^-	3.66×10^5	6.98×10^6	7.00×10^6	6.24×10^5	6.54×10^5

[a] t-Butyl salts of the respective anions were used for the studies. [b] Estimated errors were <15%. [c] NA: not applicable.

By using eq 1 the equilibrium constant K for receptor−anion interaction has been evaluated, and the values are given in Table 6.[37] It may be noted that the values of K for the receptors **1**, **3**, and **4** with F^- are roughly of 5 orders of magnitudes, while that of **2** is of 6 orders of magnitudes with F^- and AcO^-.

It was reported previously that suitably substituted H-bond donor receptor functionality undergo deprotonation in the presence of excess anions, leading to classical Brønsted acid−base chemistry, and is not commonly believed as a supramolecular interaction.[38−40] It has been argued that the higher stability of a polynuclear aggregate, such as HF_2^-, further facilitates deprotonation of the receptor unit.[38−40] To examine such a possibility, spectrophotometric titrations of the receptors were also carried out with a solution of TBAOH (Figure S10, Supporting Information). The spectral patterns for the complexes have close resemblance to the spectra of these receptors in the presence of F^- and AcO^- ions. These observations suggest that, in a large excess of anions, anion-induced deprotonation of the imidazole NH protons of the metalloreceptors occur.

Fluorescence Signaling. It has been observed in the previous section that all the complexes exhibit a moderately strong luminescence at room temperature. This means that more than one optical signal is possible, strengthening the sensing capability of the systems. Supporting Information, Figure S7 and Figure 8 show that the emission intensity of the band around the 667 nm region for **1** and **3**, 681 nm for **2**, and at 760 nm for **4**, undergoes nominal change with the addition of excess of Cl^-, Br^-, I^-, ClO_4^-, and $H_2PO_4^-$ ions, indicating the inability of these anions to deprotonate the imidazole NH protons of the metalloreceptors. On the other hand, with the ten-fold addition of the F^- ions, the emission intensity of the said band gets significantly quenched in all cases. For the receptor **2**, similar quenching of the emission intensity also occurs with AcO^- and to a lesser extent also with $H_2PO_4^-$ ions with consequent red shift of emission maximum from 681 to 781 nm. These observations are consistent with those of the absorption experiments.

Photoluminescence titrations of the receptors with various anions have been carried out in the same way as already described for spectrophotometric measurements. The effects of incremental addition of F^- and AcO^- ions to the solution of the receptors on their emission spectra are shown in Figures 9 and 10, and the insets show the quenching of luminescence intensities vs the concentration of anions added. The fluorescence titration experiments were used to determine the equilibrium constants between the receptors and the anions (Table 6), which are consistent with the results obtained from absorption data. Spectrofluorometric titrations of the complexes were also carried out with TBAOH. The spectral patterns have close resemblance to the spectra of the receptors in the presence of anions.

It is of interest to note that the position of the lowest energy MLCT band of complexes **1** and **3** showed a red-shift in their absorption spectra, while a blue-shift in their emission spectra was obtained upon addition of F^- ion. Because of the deprotonation of the imidazole NH proton, the π^* orbital of tpy-HImzphen ligand is more destabilized than the $Ru^{II}(d\pi)^6$ metal-centered orbital in the ground state complex. But in the excited state, the $Ru^{II}(d\pi)^6$ metal orbital is strongly destabilized compared with the π^* orbital of tpy-HImzphen, and in the excited state, an electronic transition occurs from the destabilized metal orbital to the π^* orbital of tpy-HImzphen (not tpy-HImzphen$^-$) resulting in a larger energy gap between $Ru^{II}(d\pi)^6$ and the π^* orbital of tpy-HImzphen causing a blue shift in emission energies.

^{1}H NMR Signaling. ^{1}H NMR spectra of the complexes (**1**−**4**) in presence of 10 equiv of F^- ions were also recorded (Figure S11 and Figure S12, Supporting Information) and the chemical shift values are collected in Table S2 (Supporting Information). The most downfield-shifted resonances that were observed between δ = 13.71 ppm and δ = 15.03 ppm in the free receptors are due to the imidazole NH proton(s), which are hydrogen bonded to $(CD_3)_2SO$. When 10 equiv of TBAF is added to the $(CD_3)_2SO$ solution of the metal complexes, complete removal of the N−H signal and upfield shift of the aromatic proton of tpy-HImzphen as well as H_2pbbzim occur. Clearly, F^- ion acts as the proton abstractor and the shielding effect is a consequence of the increase in electron density of the imidazole moiety because of the deprotonation of the N−H protons. As expected, the chemical shifts of the aromatic protons due to tpy-$PhCH_3$ ligands differ only to a small extent in the complexes.

Figure 11 shows that with the incremental addition of TBAF, the singlet at δ 15.03 ppm due to two N−H groups of H_2pbbzim is broadened, up-field shifted, and finally vanished when almost 3 equiv of F^- was added to DMSO-d_6 solution of **2**, while the chemical shifts of C−H protons of H_2pbbzim (H_{12}', H_{13}, H_{14} and H_{15}) is progressively up-field shifted. Figure S13 (Supporting Information) shows the change of chemical shifts for the above benzimidazole protons as a function of the equivalents of F^- added, and the chemical shifts values of different protons with varying amount of F^- are summarized in Table S3 (Supporting Information). The similar behavior was

dx.doi.org/10.1021/ic201610w | Inorg. Chem. 2011, 50, 12586−12600

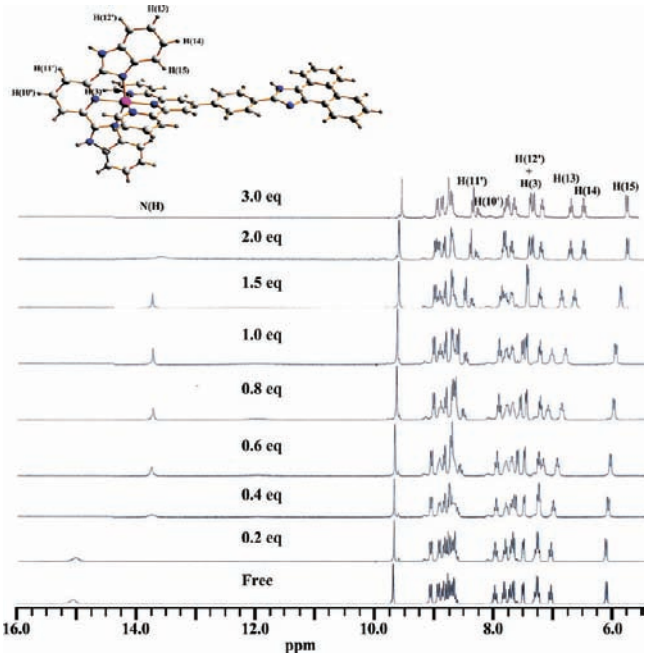

Figure 11. ^{1}H NMR (300 MHz) titration of **2** in DMSO-d_6 solution with the addition of incremental amount of F^- ion (0−3 equiv).

also found for **2** with AcO^- ions. But with $H_2PO_4^-$, the same titration was not successful because of the precipitation of the complex on addition of excess anion.

Electrochemical Signaling. The electrochemical anion recognition and sensing of the receptors as a function of different anions have been examined by using cyclic and square wave voltammetry. Incremental addition of F^- to **1**, **3**, and **4** and both F^- and AcO^- to **2** resulted in a negative shift of the oxidation potential. As shown in Figure S14 (Supporting Information), with progressive addition of F^- to **2** the current height of the redox couple observed at 0.99 V gradually diminishes and at its expense a new couple that appears at 0.44 V grows in current heights. As the F^- ion concentration reaches to 3 equiv, the couple at 0.99 V is completely replaced by the 0.44 V couple. The electrochemical behavior of **2** observed with AcO^- as the guest anion is almost identical to that of F^-. Thus, in the presence of excess of anions, imidazole NH protons are successively deprotonated thereby increasing the electron density on the metal center and causing a negative shift of the oxidation potential. It should be noted that the redox potentials of the complexes in pure acetonitrile, as reported in an earlier section, differ from those obtained in acetonitrile−dimethylformamide (9:1) medium because of solvent effect. The results presented here provide a hint that the complexes **1**−**4** could prove useful in the fabrication of electrochemical sensors.

Nature of Receptor−Anion Interaction. The observations made above from ^{1}H NMR, photometric, luminescence, and electrochemical measurements unequivocally suggest that F^- ion interacts strongly with the metalloreceptors **1**−**4**, albeit such interaction is either very weak or absent for other halides (Cl^-, Br^-, I^-) and oxyanions ($H_2PO_4^-$ and ClO_4^-). The close resemblance of both absorption and emission spectral patterns of the receptors in the presence of OH^- to those in the presence of F^- ion suggest that metal-coordinated imidazole NH protons in **1**−**4** are successively deprotonated in the presence of excess of anions. As the most electronegative atom, fluoride can form the strongest hydrogen bond with protons and tend to deprotonate polar NH groups. It has been suggested that the higher stability of a polynuclear aggregate, such as HF_2^-, facilitates the deprotonation of the receptor unit.[38−40] Thus, various colorimetric sensors containing NH arrays have been developed to detect F^- ion based on the deprotonation mechanism.[39,40] Finally, we note that although the receptor **2** exhibits strong response toward sensing F^- and AcO^-, lacking the selectivity to differentiate these anions explicitly, the other receptors (**1**, **3**, and **4**) exhibit strong selectivity toward sensing F^- ion only.

CONCLUSION

In conclusion, we have developed a new series of homo- and heteroleptic tridentate ruthenium(II) and osmium(II) complexes by using tridentate ligand, 2-(4-[2,2′:6′,2″]terpyridine-4′-yl-phenyl)-1*H*-phenanthro[9,10-*d*]imidazole (tpy-HImzphen) in combination with 2,6-bis(benzimidazole-2-yl)pyridine (H_2pbbzim) and 4′-(4-methylphenyl)-2,2′:6′,2″-terpyridine (tpy-PhCH_3), which can act as multi-channel sensors of F^- ion in solutions. To allow fine-tuning of the electronic properties, several homo- and heteroleptic complexes have been synthesized. The most striking feature of this class of compounds is that they are luminescent at room temperature in fluid solutions and their room temperature lifetimes lie in the range of 10−55 ns. The sub-nanosecond excited-state lifetime of normal tpy complexes is widely accepted as being due to the small energy gap between the emitting ^{3}MLCT state and the deactivating ^{3}MC level. The important outcome of this study is to increase the energy level separation of the two states by modulating the ^{3}MLCT energy level of the complexes by introducing extensive delocalized phenanthrene-imidazole group in the 4′-position of the tpy unit, while keeping the energy of the ^{3}MC state essentially unchanged. Another point of interest is that the spectral and redox properties of the compounds are strongly influenced by the protonation state of the imidazole rings. This opens the possibility of the application of such compounds as proton driven molecular switches. The binding properties are also confirmed by absorption, emission and ^{1}H NMR spectroscopic and cyclic voltammetric techniques. From sensing studies, it has been concluded that in the presence of excess of anions, stepwise deprotonation of the imidazole N−H fragments occurs, an event which is signaled by the development of intense and beautiful colors visible with the naked eye.

ASSOCIATED CONTENT

Supporting Information

X-ray crystallographic file in CIF format for compound **2**, **3**, and **4**. Tables **S1**−**S3** and Figures **S1**−**S14**. This material is available free of charge via the Internet at http://pubs.acs.org.

AUTHOR INFORMATION

Corresponding Author

*E-mail: sbaitalik@hotmail.com.

ACKNOWLEDGMENTS

This paper is dedicated to my mentor, Professor Kamalaksha Nag, IACS on the occasion of his 70th birthday. Financial assistance received from the Department of Science and Technology, New Delhi [Grant SR/S1/IC-33/2010] and the Council of Scientific and Industrial Research, New Delhi, India,

[Grant 01(2084)/06/EMR-II] is gratefully acknowledged. Thanks are due to the DST for providing single crystal X-ray difractometer in FIST and Time-Resolved Nanosecond Spectrofluorimeter in the PURSE programme at the Department of Chemistry of Jadavpur University. C.B., D.S., and S.D. thank CSIR for their fellowship.

REFERENCES

(1) (a) Meyer, T. J. *Pure Appl. Chem.* **1986**, *58*, 1193. (b) Juris, A.; Balzani, V.; Barigelletti, F.; Campagna, S.; Belser, P.; von Zelewsky, A. *Coord. Chem. Rev.* **1988**, *84*, 85. (c) Balzani, V.; Juris, A.; Venturi, M.; Campagna, S.; Serroni, S. *Chem. Rev.* **1996**, *96*, 759. (d) Sauvage, J.-P.; Collin, J. P.; Chambron, J. C.; Guillerez, S.; Coudret, C.; Balzani, V.; Barigelletti, F.; De Cola, L.; Flamigni, L. *Chem. Rev.* **1994**, *94*, 993.

(2) (a) Balzani, V.; Scandola, F. *Supramolecular Photochemistry*; Horwood: Chichester, U.K., 1991. (b) Balzani, V.; Credi, A.; Venturi, M. *Molecular Devices and Machines*; Wiley-VCH: Weinheim, Germany, 2003. (c) Scandola, F.; Chiorboli, C.; Indelli, M. T.; Rampi, M. A. In *Electron Transfer in Chemistry*; Balzani, V., Ed.; VCH-Wiley: Weinheim, Germany, 2001; Vol. 3, p 337. (d) Sun, L.; Hammarström, L.; Akermark, B.; Styring, S. *Chem. Soc. Rev.* **2001**, *30*, 36. (e) Wang, X.; Guerzo, A.; Baitalik, S.; Simon, G.; Shaw, G. B.; Chen, L. X.; Schmehl, R. *Photosynth. Res.* **2006**, *87*, 83. (f) Liu, Y.; DeNicola, A.; Ziessel, R.; Schanze, K. S. *J. Phys. Chem. A* **2003**, *107*, 3476. (g) Alstrum-Acevedo, J. H.; Brennaman, M. K.; Meyer, T. J. *Inorg. Chem.* **2005**, *44*, 6802. (h) Browne, W. R.; O'Boyle, N. M.; McGarvey, J. J.; Vos, J. G. *Chem. Soc. Rev.* **2005**, *34*, 641. (i) Balzani, V.; Clemente-Léon, M.; Credi, A.; Ferrer, B.; Venturi, M.; Flood, A. H.; Stoddart, J. F. *Proc. Natl. Acad. Sci. U.S.A.* **2006**, *103*, 1178. (j) Kuang, D.; Ito, S.; Wenger, B.; Klein, C.; Moser, J.-E.; Humphry-Baker, R.; Zakeeruddin, S. M.; Gratzel, M. *J. Am. Chem. Soc.* **2006**, *128*, 4146 , and references therein.

(3) (a) Keene, F. R. *Chem. Soc. Rev.* **1998**, *27*, 185. (b) Bodige, S.; Kim, M.-J.; MacDonnell, F. M. *Coord. Chem. Rev.* **1999**, *185*−*186*, 535. (c) Knof, U.; von Zelewsky, A. *Angew. Chem., Int. Ed.* **1999**, *38*, 302.

(4) (a) Constable, E. C. *Chem. Soc. Rev.* **2004**, *33*, 246. (b) Hofmeier, H.; Schubert, U. S. *Chem. Soc. Rev.* **2004**, *33*, 373−399. (c) Medlycott, E. A.; Hanan, G. S. *Coord. Chem. Rev.* **2006**, *250*, 1763. (d) Medlycott, E. A.; Hanan, G. S. *Chem. Soc. Rev.* **2005**, *34*, 133. (e) Wang, X.-Y.; Del Guerzo, A.; Schmehl, R. H. *J. Photochem. Photobiol. C* **2004**, *5*, 55. (f) Baranoff, E.; Collin, J. P.; Flamigni, L.; Sauvage, J.-P. *Chem. Soc. Rev.* **2004**, *33*, 147.

(5) Winkler, J. R.; Netzel, T.; Creutz, C.; Sutin, N. *J. Am. Chem. Soc.* **1987**, *109*, 2381.

(6) (a) Maestri, M.; Armaroli, N.; Balzani, V.; Constable, E. C.; Thompson, A. M. W. C. *Inorg. Chem.* **1995**, *34*, 2759. (b) Constable, E. C.; Cargill Thompson, A. M. W.; Armaroli, N.; Balzani, V.; Maestri, M. *Polyhedron* **1992**, *11*, 2707. (c) Wang, J.; Fang, Y. Q.; Hanan, G. S.; Loiseau, F.; Campagna, S. *Inorg. Chem.* **2005**, *44*, 5.

(7) (a) Fang, Y. Q.; Taylor, N. J.; Laverdiere, F.; Hanan, G. S.; Loiseau, F.; Nastasi, F.; Campagna, S.; Nierengarten, H.; Leize-Wagner, E.; Van Dorsselaer, A. *Inorg. Chem.* **2007**, *46*, 2854. (b) Fang, Y. Q.; Taylor, N. J.; Hanan, G. S.; Loiseau, F.; Passalacqua, R.; Campagna, S.; Nierengarten, H.; Van Dorsselaer, A. *J. Am. Chem. Soc.* **2002**, *124*, 7912.

(8) (a) Polson, M. I. J.; Loiseau, F.; Campagna, S.; Hanan, G. S. *Chem. Commun.* **2006**, 1301. (b) Passalacqua, R.; Loiseau, F.; Campagna, S.; Fang, Y. Q.; Hanan, G. S. *Angew. Chem., Int. Ed.* **2003**, *42*, 1608.

(9) (a) Encinas, S.; Flamigni, L.; Barigelletti, F.; Constable, E. C.; Housecroft, C. E.; Schofield, E. R.; Figgemeier, E.; Fenske, D.; Neuburger, M.; Vos, J. G.; Zehnder, M. *Chem.—Eur. J.* **2002**, *8*, 137. (b) Hammarström, L.; Barigelletti, F.; Flamigni, L.; Indelli, M. T.; Armaroli, N.; Calogero, G.; Guardigli, M.; Sour, A.; Collin, J.-P.; Sauvage, J.-P. *J. Phys. Chem. A* **1997**, *101*, 9061.

(10) (a) Hissler, M.; El-ghayoury, A.; Harriman, A.; Ziessel, R. *Angew. Chem., Int. Ed.* **1998**, *37*, 1717−1720. (b) Benniston, A. C.; Grosshenny, V.; Harriman, A.; Ziessel, R. *Angew. Chem., Int. Ed.* **1994**, *33*, 1884−1885. (c) Benniston, A. C.; Harriman, A.; Li, P.; Sams, C. A. *J. Am. Chem. Soc.* **2005**, *127*, 2553−2564. (d) Baitalik, S.; Wang, X.; Schmehl, R. H. *J. Am. Chem. Soc.* **2004**, *126*, 16304−16305. (e) Wang, X-y.; Del Guerzo, A.; Tunuguntla, H.; Schmehl, R. H. *Res. Chem. Intermed.* **2007**, *33*, 63.

(11) (a) Duati, M.; Tasca, S.; Lynch, F. C.; Bohlen, H.; Vos, J. G.; Stagni, S.; Ward, M. D. *Inorg. Chem.* **2003**, *42*, 8377. (b) Duati, M.; Fanni, S.; Vos, J. G. *Inorg. Chem. Commun.* **2000**, *3*, 68.

(12) (a) Indelli, M. T.; Bignozzi, C. A.; Scandola, F.; Collin, J.-P. *Inorg. Chem.* **1998**, *37*, 6084. (b) Constable, E. C.; Dunne, S. J.; Rees, D. G. F.; Schmitt, C. X. *Chem. Commun.* **1996**, 1169.

(13) (a) Beley, M.; Collin, J.-P.; Louis, R.; Metz, B.; Sauvage, J.-P. *J. Am. Chem. Soc.* **1991**, *113*, 8521. (b) Beley, M.; Collin, J.-P.; Sauvage, J.-P. *Inorg. Chem.* **1993**, *32*, 4539. (c) Wilkinson, A. J.; Puschmann, H.; Howard, J. A. K.; Foster, C. E.; Williams, J. A. G. *Inorg. Chem.* **2006**, *45*, 8685. (d) Beley, M.; Chodorowski, S.; Collin, J.-P.; Sauvage, J.-P.; Flamigni, L.; Barigelletti, F. *Inorg. Chem.* **1994**, *33*, 2543. (e) Wadman, S. H.; Lutz, M.; Tooke, D. M.; Spek, A. L.; Hartl, F.; Havenith, R.W. A.; van Klink, G. P. M.; van Koten, G. *Inorg. Chem.* **2009**, *48*, 1887.

(14) (a) Abrahamsson, M.; Lundqvist, M. J.; Wolpher, H.; Johansson, O.; Eriksson, L.; Bergquist, J.; Rasmussen, T.; Becker, H.-C.; Hammarström, L.; Norrby, P.-O.; Åkermark, B.; Persson, P. *Inorg. Chem.* **2008**, *47*, 3540. (b) Abrahamsson, M.; Jäger, M.; Österman, T.; Eriksson, L.; Persson, P.; Becker, H. C.; Johansson, O.; Hammarström, L. *J. Am. Chem. Soc.* **2006**, *128*, 12616. (c) Abrahamsson, M.; Jäger, M.; Kumar, R. J.; Österman, T.; Persson, P.; Becker, H. C.; Johansson, O.; Hammarström, L. *J. Am. Chem. Soc.* **2008**, *130*, 15533.

(15) Sessler, J. L.; Gale, P. A.; Cho, W. S. *Anion Receptor Chemistry*; Royal Society of Chemistry: Cambridge, U.K., 2006.

(16) (a) Beer, P. D.; Bayly, S. R. *Top. Curr. Chem.* **2005**, *255*, 125. (b) Caltagirone, C.; Gale, P. A. *Chem. Soc. Rev.* **2009**, *38*, 520. (c) Gale, P. A. *Coord. Chem. Rev.* **2006**, *250*, 2917. (d) Sessler, J. L.; Davis, J. M. *Acc. Chem. Res.* **2001**, *34*, 989. (e) Quang, D. T.; Kim, J. S. *Chem. Rev.* **2007**, *107*, 3780. (f) Mutihac, L.; Lee, J. H.; Kim, J. S.; Vicens, J. *Chem. Soc. Rev.* **2011**, *40*, 2777.

(17) Martínez-Máñez, R.; Sancenón, F. *Chem. Rev.* **2003**, *103*, 4419.

(18) Steed, J. W. *Chem. Soc. Rev.* **2009**, *38*, 506.

(19) (a) dos Santos, C. M. G.; Harte, A. J.; Quinn, S. T.; Gunnalaugsson, T. *Coord. Chem. Rev.* **2008**, *252*, 2512. (b) Gunnalaugsson, T.; Glynn, M.; Tocci, (nee Hussey), G. M.; Kruger, P. E.; Pfeffer, F. M. *Coord. Chem. Rev.* **2006**, *250*, 3094.

(20) (a) Peŕez, J.; Riera, L. *Chem. Commun.* **2008**, 533. (b) Peŕez, J.; Riera, L. *Chem. Soc. Rev.* **2008**, *37*, 2658.

(21) (a) Rice, C. R. *Coord. Chem. Rev.* **2006**, *250*, 3190. (b) Kumar, A.; Sun, S.-S.; Lees, A. J. *Coord. Chem. Rev.* **2008**, *252*, 922. (c) Amendola, V.; Gómez, E. D.; Fabbrizzi, L.; Licchelli, M. *Acc. Chem. Res.* **2006**, *39*, 343. (d) Suksai, C.; Tuntulani., T. *Top. Curr. Chem.* **2005**, *255*, 163. (e) Amendola, V.; Fabbrizzi, L. *Chem. Commun.* **2008**, 513.

(22) (a) Bhaumik, C.; Das, S.; Saha, D.; Dutta, S.; Baitalik, S. *Inorg. Chem.* **2010**, *49*, 5049. (b) Saha, D.; Das, S.; Maity, D.; Dutta, S.; Baitalik, S. *Inorg. Chem.* **2011**, *50*, 46. (c) Saha, D.; Das, S.; Bhaumik, C.; Dutta, S.; Baitalik, S. *Inorg. Chem.* **2010**, *49*, 2334. (d) Das, S.; Saha, D.; Bhaumik, C.; Dutta, S.; Baitalik, S. *Dalton Trans.* **2010**, *39*, 4162.

(23) (a) Yam, V. W. W. *Acc. Chem. Res.* **2002**, *35*, 555. (b) Wong, K. M. C.; Tang, W. S.; Lu, X. X.; Zhu, N.; Yam, V. W. W. *Inorg. Chem.* **2005**, *44*, 1492. (c) Yam, V. W. W.; Tang, R. P. L.; Wong, K. M. C.; Lu, X. X.; Cheung, K. K.; Zhu, N. *Chem.—Eur. J.* **2002**, *8*, 4066. (d) Yam, V. W. W.; Wong, K. M. C.; Zhu, N. *Angew. Chem., Int. Ed.* **2003**, *42*, 1400.

(24) (a) Anzebacher, P.; Tyson, D. S.; Jurslkova, K.; Castellano, F. N. *J. Am. Chem. Soc.* **2002**, *124*, 6232. (b) Mizuno, T.; Wei, W.-H.; Eller, L. R.; Sessler, J. L. *J. Am. Chem. Soc.* **2002**, *124*, 1134. (c) Beer, P. D.; Szemes, F.; Balzani, V.; Salà, C. M.; Drew, M. G. B.; Dent, S. W.; Maestri, M. *J. Am. Chem. Soc.* **1997**, *119*, 11864. (d) Cui, Y.; Mo, H.-J.; Chen, J.-C.; Niu, Y.-L.; Zhong, Y.-R.; Zheng, K.-C.; Ye, B.-H. *Inorg. Chem.* **2007**, *46*, 6427. (e) Lin, Z.-H.; Zhao, Y.-G.; Duan, C.-Y.; Zhang, B.-G.; Bai, Z.-P. *Dalton Trans.* **2006**, 3678. (f) Ion, L.; Morales, D.; Perez, J.; Riera, L.; Riera, V.; Kowenicki, R. A.; McPartlin, M. *Chem.*

Commun. **2006**, 91. (g) Zapata, F.; Caballero, A.; Espinosa, A.; Tárraga, A.; Molina, P. *J. Org. Chem.* **2008**, *73*, 4034. (h) Derossi, S.; Adams, H.; Ward, M. D. *Dalton Trans.* **2007**, 33. (i) Lin, T.-P.; Chen, C.-Y.; Wen, Y.-S.; Sun, S.-S. *Inorg. Chem.* **2007**, *46*, 9201.

(25) Spahni, W.; Calzaferri, G. *Helv. Chim. Acta* **1984**, *67*, 450.

(26) Pott, K. T.; Usifer, D. A.; Abruna, H. D. *J. Am. Chem. Soc.* **1987**, *109*, 3961−3967.

(27) (a) Addison, A. W.; Burke, P. *J. Heterocycl. Chem.* **1981**, *18*, 803−805. (b) Addison, A. W.; Rao, T. N.; Wahlgren, C. G. *J. Heterocycl. Chem.* **1983**, *20*, 1481−1484.

(28) Schneider, H.-J.; Yatsimirsky, A. *Principles and Methods in Supramolecular Chemistry*; John Wiley & Sons: Chichester, England, 2000; p 142.

(29) *SAINT* (version 6.02), *SADABS* (version 2.03); Bruker AXS Inc.: Madison, WI, 2002.

(30) Sheldrick, G. M. *SHELXL-97, Program for the Refinement of crystal Structures*; University of Göttingen: Göttingen, Germany, 1997.

(31) *SHELXTL*, version 6.10; Bruker AXS Inc.: Madison, WI, 2002.

(32) *PLATON*; Spek, A. L. *J. Appl. Crystallogr.* **2003**, *36*, 7−13.

(33) (a) Coe, B. J.; Thompson, D. W.; Culbertson, C. T.; Schoonover, J. R.; Meyer, T. J. *Inorg. Chem.* **1995**, *34*, 3385. (b) Kober, E. M.; Meyer, T. J. *Inorg. Chem.* **1982**, *21*, 3967.

(34) (a) Xiaoming, X.; Haga, M.; Inoue, T. M.; Ru, Y.; Addison, A. W.; Kano, K. *J. Chem. Soc., Dalton Trans.* **1993**, 2477. (b) Haga, M.; Takasugi, T.; Tomie, A.; Ishizuya, M.; Yamada, T.; Hossain, M. D.; Inoue, M. *Dalton Trans.* **2003**, 2069.

(35) (a) Liu, Y.; Hammitt, R.; Lutterman, D. A.; Thummel, R. P.; Turro, C. *Inorg. Chem.* **2007**, *46*, 6011. (b) Liu, Y.; Hammitt, R.; Lutterman, D. A.; Joyce, L. E.; Thummel, R. P.; Turro, C. *Inorg. Chem.* **2009**, *48*, 375.

(36) (a) Vogler, L. M.; Brewer, K. J. *Inorg. Chem.* **1996**, *35*, 818. (b) Arana, C. R.; Abruña, H. D. *Inorg. Chem.* **1993**, *32*, 194.

(37) Attempts to determine the binding constants of the complexes for anions with 1:2 stoichiometry did not result in any satisfactory fit. The binding constants were obtained by fitting the data to two successive 1:1 equilibrium processes using equation 1.

(38) (a) Kang, S. O.; Powell, D.; Day, V. W.; Bowman-James, K. *Angew. Chem., Int. Ed.* **2006**, *45*, 7882. (b) Gunnlaugasson, T.; Kruger, P. E.; Jensen, P.; Tierney, J.; Ali, H. D. P.; Hussey, G. M. *J. Org. Chem.* **2005**, *70*, 10875. (c) dos Santos, C. M. G.; Gunnlaugsson, T. *Dalton Trans.* **2009**, 4712. (d) Peng, X.; Wu, Y.; Fan, J.; Tian, M.; Han, K. *J. Org. Chem.* **2005**, *70*, 10524.

(39) (a) Gomez, D. E.; Fabbrizzi, L.; Licchelli, M. *J. Org. Chem.* **2005**, *70*, 5717. (b) Boiocchi, M.; Boca, L. D.; Gomez, D. E.; Fabbrizzi, L.; Licchelli, M.; Monzani, E. *Chem.—Eur. J.* **2005**, *11*, 3097. (c) Amendola, V.; Boiocchi, M.; Fabbrizzi, L.; Palchetti, A. *Chem.—Eur. J.* **2005**, *11*, 5648. (d) Amendola, V.; Boiocchi, D.; Colasson, B.; Fabbrizzi, L. *Inorg. Chem.* **2006**, *45*, 6138.

(40) (a) Nishiyabu, R.; Anzenbacher, P. Jr. *J. Am. Chem. Soc.* **2005**, *127*, 8270. (b) Aldakov, D.; Palacios, M. A.; Anzenbacher, P. *Chem. Mater.* **2005**, *17*, 5238.